

A VELOCITY-ENTROPY INVARIANCE THEOREM FOR THE CHAPMAN-JOUGUET DETONATION

Pierre Vidal and Ratiba Zitoun

Institut Pprime, UPR 3346 CNRS,
BP40109, 86961 Futuroscope-Chasseneuil, FRANCE

June 20, 2020

The velocity and the specific entropy of the Chapman-Jouguet (CJ) equilibrium detonation in a homogeneous explosive are shown to be invariant under the same variations of the initial pressure and temperature. The CJ state and isentrope can then be defined from the CJ velocity or, conversely, the CJ velocity from one CJ variable, without equation of state for detonation products. For gaseous explosives, comparison to calculations with detailed chemical equilibrium shows agreement to within $\mathcal{O}(0.1)$ %. However, the CJ pressures of four carbonate liquid explosives are found about 20 % larger than measured values: the CJ-equilibrium model appears not to apply to condensed carbonate explosives, which supports a former conclusion by Davis, Craig and Ramsay, although for the opposite reason. A simple hydrodynamic criterion for assessing the representativeness of this CJ model is thus proposed, which nevertheless cannot determine which of its assumptions may not be satisfied, namely CJ equilibrium, single-phase fluid, and laminar flow. This invariance might be an illustration of a general feature of hyperbolic systems and their characteristic surfaces.

1. Introduction	2
2. Reminders and notation	3
2.1 Where the Chapman-Jouguet model lies	3
2.2 Thermodynamic and hydrodynamic relations	4
2.3 Chapman-Jouguet states and velocities, and a remark	5
3. A Velocity-Entropy invariance theorem	7
3.1 The initial-variations problem	7
3.2 Rankine-Hugoniot differentials	8
3.3 Demonstration and interpretation	10
3.4 Chapman-Jouguet supplemental properties	11
4. Application to gaseous or liquid explosives	16
4.1 Gaseous explosives with ideal final states	16
4.2 Liquid explosives	21
5. Discussion and conclusions	24
Appendix A. Perfect-gas relations	25
Appendix B. Chapman-Jouguet admissibility	26
Appendix C. A model problem	27
References	28

1. Introduction

1. The Chapman-Jouguet (CJ) detonation [1] is a classic of combustion theory. It is defined as the fully-reactive, planar and compressive discontinuity wave, with velocity constant, supersonic with respect to the initial state, and sonic with respect to the final burnt state at chemical equilibrium. The CJ state and velocity are thus obtained from the Rankine-Hugoniot relations and the equation of state of detonation products. Although their representativeness is now accepted as uncertain, because detonation dynamics is unstable and quite sensitive to losses, the CJ model remains the staple of detonation theory to obtain simply reference velocities and reaction-end states: CJ properties are a limit predictable independently of any condition for detonation existence. It is the purpose of this study to bring out and investigate two CJ supplemental properties that are perhaps useful to help interpret experiments and improve modelling.

2. The first one is that the CJ detonation velocity D_{CJ} and the specific entropy s_{CJ} of a homogenous explosive substance are invariant under the same variations of the initial temperature T_0 and pressure p_0 : if one is invariant, so is the other; different initial states producing the same D_{CJ} produce different CJ states on the same isentrope. The second one is that a CJ state and its isentrope can then be calculated simply from the value of D_{CJ} without equilibrium equation of state; conversely, D_{CJ} can be obtained from one CJ variable. These results apply only to explosives whose fresh and burnt states obey thermodynamic relationships for single-phase inviscid fluids, with temperature T and pressure p as independent variables. Figure 1 depicts the CJ model and the Velocity-Entropy invariance (DSI) theorem in the Pressure (p) - Volume (v) plane based on usual properties of detonation modelling (Sect.2).

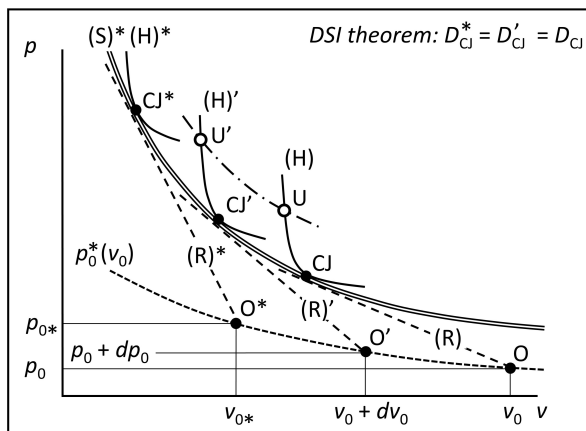


Figure 1: An equilibrium isentrope (S)* of detonation products can be the common envelope of equilibrium Hugoniot curves (H)*, (H)' and (H) and Rayleigh-Michelson lines (R)*, (R)' and (R) if their poles O*, O' and O lie on a specific $p_0^*(v_0)$ line through a reference initial state O*(p_{0*}, v_{0*}) (the Hugoniot curvatures are accentuated).

The slopes $-(D_{CJ}/v_0)^2$ of these (R) lines increase with increasing initial volume v_0 , but the DSI theorem ensures they have the same CJ velocity D_{CJ} . This determines the CJ*, CJ' and CJ states, the $p_0^*(v_0)$ initial states, and the isentrope (S)*, given D_{CJ} and the initial sound speeds and Gruneisen coefficients.

3. To some degree, this extends the Inverse Method of Jones, Stanyukovich and Manson [2], [3], [4]. This method gives the CJ hydrodynamic variables from experimental values of D_{CJ} and its derivatives with respect to two independent initial-state variables, such as p_0 and T_0 ; the present analysis shows that the only value of D_{CJ} is sufficient. Is the detonation regime identifiable from experimental detonation velocities and pressures? Models are usually rejected if they cannot represent observations, but experiments may not represent the model assumptions, differences may indicate unprecise measurements or unphysical parameters, and agreement should not exclude fewer assumptions. Equations of state of detonation products are calibrated by fitting calculated CJ properties to experimental values, although there is no criterion to ensure that the latter are those of the CJ-equilibrium detonation: this study proposes that they are not if they do not satisfy the supplemental properties.

4. Section 2 is a reminder on classical but necessary elements that also introduces the main notation, Section 3 sets out the DSI theorem and the CJ supplemental properties, Section 4 is an analysis of their agreements or differences with calculations or measurements for gases and liquids, and Section 5 is a summary with some speculative conclusions.

2. Reminders and notation

5. The CJ postulate is that the sonic and equilibrium constraints are achieved at the same position in the flow, which in fact is more of an ideal mathematical limit than an observable physical reality. The traditional introduction to this old issue is based on the Zel'dovich-von Neuman-Döring (ZND) detonation model, that is, a leading shock sustained by a subsonic laminar reaction zone [5]. The ZND model uses the frozen sound speed, the CJ model uses the equilibrium sound speed, discussions bear on which best characterizes the relative velocity of the sonic front necessary to protect the reaction zone from the rear expansion, depending on the interplay between flow dynamics and physical processes.

2.1 Where the Chapman-Jouguet model lies

6. Most explosive devices have finite transverse dimensions, so self-sustained detonations are non-ideal, with diverging reaction zones that encompass a frozen sonic locus, hence curved leading shocks and velocities lower than the planar CJ one: the flow behind the sonic locus cannot sustain the shock. However, not any reaction process can achieve CJ equilibrium as the steady planar limit of a sonic curved detonation [6]. A presentation of equilibrium-frozen issues and several non-ideal detonations was given by Higgins [7]. Heat production by physicochemical processes, possibly non-monotonic, exothermic or endothermic [8], [9], and losses by heat transfer, friction or transverse expansion of the reaction zone must offset each other at the sonic locus in order that the flow derivatives remain finite there. The dynamics of a self-sustained detonation is thus described by an eigenconstraint between the parameters of the leading-shock, that is, its normal velocity, acceleration and curvature [10], [11], [12], [13], and those of the reaction and loss rates [14]. Achieving CJ equilibrium at least requires that set-ups be wide enough so the detonation front is essentially planar and losses negligible, and that detonation run distances from ignition be large enough so the flow gradients of the expanding products are small enough to allow for a continuous equilibrium shift and, therefore, the equilibrium-sonic solution at reaction end.

7. Reaction processes differ for gases and liquids. In gases, the translational, rotational and vibrational degrees of freedom are considered to re-equilibrate much faster than chemical kinetics, thus the only process at work. In liquids, molecular-bond breaking makes the time of vibrational deexcitation comparable to that of chemical relaxation [15]. An introduction to the Non-Equilibrium ZND model was given by Tarver [16]. Local thermodynamic equilibrium would be achieved before chemical transformation in gases but perhaps not in the detonation products of liquids, and actually of most condensed explosives, also considering its interplay with the endothermic aggregation of solid carbon particles, a process accepted as inherent to detonation in carbonate condensed explosives [17] p.186-190, [18], [19]. The DSI theorem is restricted to detonation products described as a single-phase fluid at chemical equilibrium.

8. The main criticism to the ZND frame of analysis for homogeneous explosive is the instability of their reaction zones: they are not laminar, and detonation fronts have a three-dimensional structure. In gases, the flow advects unburnt pockets, the front has a cellular structure, and the experimental mean widths of detonation cells are 10 to 50 times greater than calculated characteristic thicknesses of planar steady ZND reaction zones [20], [21], even if such widths may be difficult to define. In liquids, instabilities have been often observed, but how they relate to chemical kinetics and whether they are similar to those in gases is still being investigated [19], [22], [23], [24], [25] (and refs. therein). The surface areas of the detonation front or the cross section of the experimental device at least must be large enough compared to the mean width of the instabilities for the CJ properties can be considered as representative averages.

9. The CJ supplemental properties in this work do not aim at indicating which of the CJ assumptions may not be satisfied, namely sonic-equilibrium, single-phase fluid, or laminar flow. However, they do not draw on any particular equation of state, so they provide a simple hydrodynamic criterion for determining whether experimental and numerical data are representative of the CJ-equilibrium model.

2.2 Thermodynamic and hydrodynamic relations

10. Single-phase inviscid fluids, whether inert or at chemical equilibrium, have two basic independent state variables, namely temperature T and pressure p , but specific volume $v(T, p)$ is more convenient than T for hydrodynamics because it appears explicitly in the balance equations. Specific enthalpy h and entropy s are the main state functions used in this work; their differentials write

$$dh(s, p) = Tds + vdp, \quad dh(p, v) = \frac{G+1}{G}vdp + \frac{c^2}{G}\frac{dv}{v}, \quad (1)$$

$$dh(T, p) = C_p dT + \left(1 - \frac{T}{v} \frac{\partial v}{\partial T}\right)_p vdp, \quad Tds(p, v) = \frac{vdp}{G} + \frac{c^2}{G}\frac{dv}{v}, \quad (2)$$

$$c^2 = Gv \left(\frac{\partial h}{\partial v}\right)_p = -v^2 \left(\frac{\partial p}{\partial v}\right)_s, \quad G = \frac{v}{\left(\frac{\partial h}{\partial p}\right)_v - v} = -\frac{v}{T} \left(\frac{\partial T}{\partial v}\right)_s, \quad (3)$$

where c is the sound speed, G is the Gruneisen coefficient and C_p is the heat capacity at constant pressure. In gases, the adiabatic exponent γ defines the convenient representation of c

$$c^2 = \gamma pv, \quad \gamma = -\frac{v}{p} \left(\frac{\partial p}{\partial v}\right)_s. \quad (4)$$

In the p - v plane, isentropes ($ds = 0$) have negative slopes since $\gamma > 0$, and their local convexities are defined by the sign of the fundamental derivative of hydrodynamics Γ [26], [27], [28], [29] (most fluids have uniformly convex isentropes: $\Gamma > 0$, their slopes monotonically decrease with increasing volume),

$$\Gamma = \frac{1}{2} \frac{v^3}{c^2} \left(\frac{\partial^2 p}{\partial v^2}\right)_s = \frac{-v}{2} \left(\frac{\partial^2 p}{\partial v^2}\right)_s / \left(\frac{\partial p}{\partial v}\right)_s = 1 - \frac{v}{c} \left(\frac{\partial c}{\partial v}\right)_s. \quad (5)$$

11. The fresh (initial, subscript 0) and the equilibrium (final, no subscript) states of a reactive medium have different state functions and coefficients because their chemical compositions are different. Typically, $\gamma < \gamma_0$ and, if products are brought from a (T, p) equilibrium state to the (T_0, p_0) initial state, $v(T_0, p_0) > v_0 = v_0(T_0, p_0)$ and $h(T_0, p_0) < h_0 = h_0(T_0, p_0)$. The difference of enthalpies $Q_0 = h_0(T_0, p_0) - h(T_0, p_0)$ at (T_0, p_0) is the heat of reaction at constant pressure.

12. Conservation of mass, momentum and energy surface fluxes through hydrodynamic discontinuities is expressed by the Rankine-Hugoniot relations, which, along the normal to the discontinuity, write

$$\rho_0 D = \rho(D - u), \quad p_0 + \rho_0 D^2 = p + \rho(D - u)^2, \quad h_0 + \frac{1}{2} D^2 = h + \frac{1}{2} (D - u)^2, \quad (6)$$

where $\rho = 1/v$ is the specific mass, and u and D are the material speed and the discontinuity velocity in a laboratory-fixed frame, with initial state at rest ($u_0 = 0$). These relations combined with an $h(p, v)$ equation of state (1-b) are not a closed system since there are 4 equations for the 5 variables v, p, h, u and D , given an initial state (p_0, v_0) and $h_0(p_0, v_0)$, hence a one-variable solution, for example

$$p, v, h, u, T, s, c, \gamma, \Gamma, G, \dots \equiv \eta(D; v_0, p_0). \quad (7)$$

13. Its representation in the p - v plane (Fig.2) is an intersect of a Rayleigh-Michelson (R) line $p_R(v; D; v_0, p_0)$ and the Hugoniot (H) curve $p_H(v; v_0, p_0)$, namely

$$p_R : p = p_0 + \left(\frac{D}{v_0}\right)^2 (v_0 - v), \quad p_H : h(p, v) = h_0(p_0, v_0) + \frac{1}{2} (p - p_0)(v_0 + v). \quad (8)$$

A Hugoniot for a detonation ($Q_0 > 0$, $v(T_0, p_0) > v_0$) lies above that for a shock ($Q_0 = 0$, $v(T_0, p_0) = v_0$): most fluids have uniformly-convex Hugoniots with 1 compressive intersect (N, $v/v_0 < 1$) if $Q_0 = 0$ regardless of D , and 2 (U and L) if $Q_0 > 0$ and D is large enough (Fig.2-left). The observability of states on non-uniformly-convex Hugoniots is an open debate on whether theoretical instability criteria are met in Nature, based on linear and non-linear stability analyses of discontinuities [30], [31], [32], [33], [34]. At least physical admissibility (the discontinuity increases entropy, $s \geq s_0$) or equivalently mathematical determinacy (uniqueness and continuous dependence of (7) on the flow boundaries) must be satisfied [35], [36], [37]. Denoting by M_0 and M the discontinuity Mach numbers relative to the initial and the final states, this is expressed by the subsonic-supersonic evolution condition

$$u + c \geq D \geq c_0 \quad \Leftrightarrow \quad \frac{D}{c_0} = M_0 \geq 1 \geq M = \frac{D - u}{c}. \quad (9)$$

2.3 Chapman-Jouguet states and velocities, and a remark

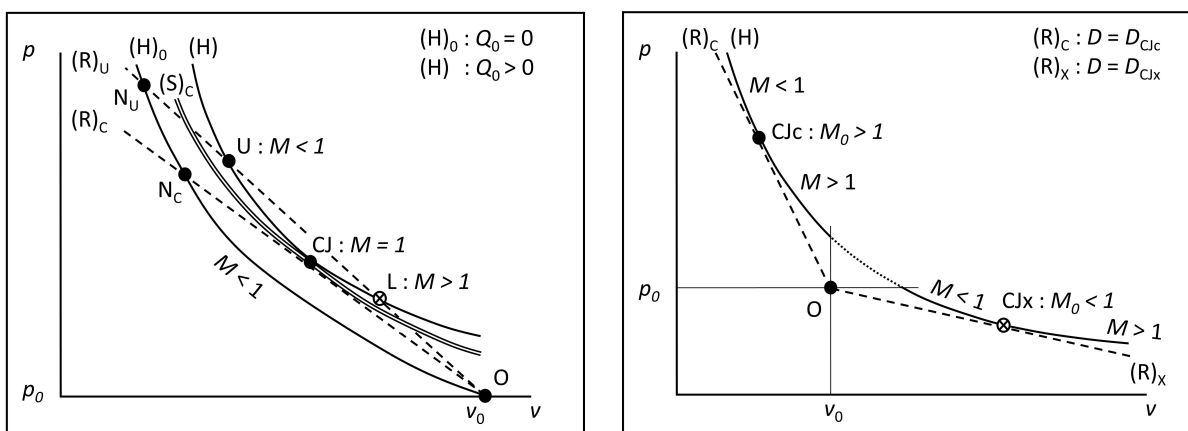


Figure 2. Left: Unreacted $(H)_0$ and equilibrium (H) Hugoniot curves, and Rayleigh-Michelson (R) lines, $(R)_U$ and $(R)_C$, for discontinuity velocities greater than or equal to D_{CJ} . Physical intersects are points N, U and CJ ($M \leq 1 \leq M_0$), the CJ isentrope $(S)_C$ is positioned between the $(R)_C$ line and the (H) curve. **Right:** detonation (upper) and deflagration (lower) Hugoniot arcs; the physical branch is above the compressive CJ point CJ_c .

14. The tangency of a Rayleigh-Michelson line $p_R(v; D)$, an equilibrium Hugoniot $p_H(v)$ and an isentrope $p_S(v)$ defines CJ points and is equivalent to the sonic condition (12) below, as shown by

$$\left. \frac{\partial p_R}{\partial v} \right)_{D, p_0, v_0} = - \left(\frac{D}{v_0} \right)^2 < 0, \quad \left. \frac{\partial p_S}{\partial v} \right)_s = - \left(\frac{D}{v_0} \right)^2 \times M^{-2} < 0, \quad (10)$$

$$\left. \frac{\partial p_H}{\partial v} \right)_{p_0, v_0} = - \left(\frac{D}{v_0} \right)^2 \times \left(1 + 2 \frac{M^{-2} - 1}{F} \right), \quad F(G, v; v_0) = 2 - G \left(\frac{v_0}{v} - 1 \right), \quad (11)$$

$$M_{CJ} = \left(\frac{D - u}{c} \right)_{CJ} = 1 \quad \text{or} \quad D_{CJ} = (u + c)_{CJ}. \quad (12)$$

There are at least 2 CJ points, such as on uniformly-convex Hugoniots (Fig.2-right). The upper, compressive, one (CJ_c) is the CJ detonation, with minimum velocity supersonic with respect to the initial state ($v_{CJ}/v_0 < 1$, $p_{CJ}/p_0 > 1$, $D_{CJc}/c_0 > 1$). The lower, expansive, one (CJ_x) is the CJ deflagration, with maximum velocity subsonic with respect to the initial state ($v_{CJ}/v_0 > 1$, $p_{CJ}/p_0 < 1$, $D_{CJx}/c_0 < 1$).

15. The admissibility of the CJ detonation requires that $\Gamma_{\text{CJ}} > 0$, which implies that $F > 0$ about and at a CJ point, that the physical branch of an equilibrium Hugoniot arc is convex and above the CJ point as M decreases from 1 and s increases with decreasing v , and that $p_{\text{S}}(v)$ is positioned between $p_{\text{H}}(v)$ and $p_{\text{R}}(v)$ if $G > 0$ (App.B). The other properties useful here are $0 \leq \partial s_{\text{H}}/\partial D)_{p_0, v_0} < \infty$ regardless of M , and, since $F_{\text{CJ}} \neq 0$, $\partial s_{\text{H}}/\partial v)_{p_0, v_0}^{\text{CJ}} = 0$ and $\partial D/\partial v)_{p_0, v_0}^{\text{CJ}} = 0$, as shown by

$$\left. \frac{v_0 T}{D^2} \frac{\partial s_{\text{R}}}{\partial v} \right)_{D, p_0, v_0} = \frac{v}{v_0} \frac{M^{-2} - 1}{G}, \quad \left. \frac{v_0 T}{D^2} \frac{\partial s_{\text{H}}}{\partial v} \right)_{p_0, v_0} = - \left(1 - \frac{v}{v_0} \right) \frac{M^{-2} - 1}{F}, \quad (13)$$

$$\left. \frac{T}{D} \frac{\partial s_{\text{H}}}{\partial D} \right)_{p_0, v_0} = \left(1 - \frac{v}{v_0} \right)^2 > 0, \quad \left. \frac{v_0}{D} \frac{\partial D}{\partial v} \right)_{p_0, v_0} = - \left(1 - \frac{v}{v_0} \right)^{-1} \frac{M^{-2} - 1}{F}. \quad (14)$$

16. The CJ condition (12) closes system (1-b)-(6): the one-variable solution (7) and (12) give the CJ velocities D_{CJ} and variables $\eta_{\text{CJ}} = (p, v, h, u, T, s, c, \gamma, \Gamma, G, \dots)_{\text{CJ}}$ as functions of the initial state,

$$D_{\text{CJ}} = D_{\text{CJ}}(v_0, p_0), \quad \eta_{\text{CJ}} = \eta_{\text{CJ}}(v_0, p_0). \quad (15)$$

Explicit solutions can be obtained with simple $h(p, v)$ equations of state (App.A). In practice, CJ detonation properties are calculated numerically by means of thermochemical codes that implement physical equilibrium equations of state and thermodynamic properties at high pressures and temperatures.

17. The hydrodynamic variables $z = (p, v, u, c)$ at CJ points have a well-known two-variables representation as functions of D_{CJ} and γ_{CJ}

$$z_{\text{CJ}} = z_{\text{CJ}}(D_{\text{CJ}}, \gamma_{\text{CJ}}; v_0, p_0), \quad (16)$$

that is, D_{CJ} can be expressed as a function of two CJ variables, for example $D_{\text{CJ}}(v_{\text{CJ}}, \gamma_{\text{CJ}}; v_0, p_0)$: the mass balance (6-a) and the R relation (8-a) combined with (4) and the CJ condition (12) thus give

$$\frac{v_{\text{CJ}}}{v_0} = \frac{c_{\text{CJ}}}{D_{\text{CJ}}} = \frac{\gamma_{\text{CJ}}}{\gamma_{\text{CJ}} + 1} \left(1 + \frac{p_0 v_0}{D_{\text{CJ}}^2} \right), \quad \frac{v_0 p_{\text{CJ}}}{D_{\text{CJ}}^2} = \frac{1 + \frac{p_0 v_0}{D_{\text{CJ}}^2}}{\gamma_{\text{CJ}} + 1}, \quad \frac{u_{\text{CJ}}}{D_{\text{CJ}}} = \frac{1 - \gamma_{\text{CJ}} \frac{p_0 v_0}{D_{\text{CJ}}^2}}{\gamma_{\text{CJ}} + 1}; \quad (17)$$

the Hugoniot relation (8-b) then gives h_{CJ} . Thus, it can be observed that the zero-variable representation (15) is obtained from a complete set that includes the energy balance and an explicit equation of state, hence the two-variables representation (16) since it does not use these 2 relations: γ_{CJ} is simply a substitute to c_{CJ} . The DSI theorem (Sect.3) supplements (16) by including the energy balance: its primary consequence is that z_{CJ} and γ_{CJ} are explicit one-variable functions of D_{CJ} (Subsection 3.4),

$$z_{\text{CJ}} = z_{\text{CJ}}(D_{\text{CJ}}; v_0, p_0), \quad \gamma_{\text{CJ}} = \gamma_{\text{CJ}}(D_{\text{CJ}}; v_0, p_0), \quad (18)$$

hence, conversely, D_{CJ} is a function of one CJ variable, for example $D_{\text{CJ}}(\gamma_{\text{CJ}}; v_0, p_0)$. The NASA computer program CEA [38] for calculating chemical equilibria in ideal gases is used in Subsection 4.1 for investigating the theorem and generating CJ properties for comparison to the theoretical ones (18).

3. A Velocity-Entropy invariance theorem

18. Considering different initial states of the same homogeneous explosive, equivalent statements are:

1. the CJ velocity D_{CJ} and specific entropy s_{CJ} are invariant under the same initial variations;
2. CJ detonations with the same D_{CJ} have the same s_{CJ} , and conversely;
3. different initial states chosen so that D_{CJ} is invariant determine different CJ states that lie on the same isentrope;
4. an isentrope is the common envelope of Hugoniot curves and Rayleigh-Michelson lines of CJ detonations that have the same velocity;
5. the variations of D_{CJ} and s_{CJ} are proportional to each other:

$$D_{\text{CJ}} = D_{\text{CJ}}(s_{\text{CJ}}), \quad \text{so} \quad dD_{\text{CJ}} \propto ds_{\text{CJ}} \quad \text{or} \quad dD_{\text{CJ}} = 0 \Leftrightarrow ds_{\text{CJ}} = 0. \quad (19)$$

The CJ state is then the solution to the system of compatibility constraints on these initial variations. The subsections below detail the initial-variations problem, the Rankine-Hugoniot differentials, the theorem demonstration and its geometrical interpretation (Fig.1), and the CJ supplemental properties.

3.1 The initial-variations problem

19. The simplest flow behind a planar discontinuity is ahead of a piston with a constant speed u_p . The flow is constant-state and subsonic, regardless of u_p behind a shock with same initial and final composition, but only if u_p is greater than the CJ material speed u_{CJ} (17-c) behind a detonation with final state at chemical equilibrium. This case defines the constant-velocity, overdriven detonation. The discontinuity velocity D and all final-state variables $\eta = (p, v, h, u, T, s, c, \gamma, \Gamma, G, \dots)$, where $u = u_p$, are then one-variable functions (Subsect.2.2), such as $D(u; v_0, p_0)$ and $\eta(u; v_0, p_0)$, or, equivalently, $\eta(D; v_0, p_0)$ (7), for example (96) (App.A). If u_p is smaller than u_{CJ} , the flow is expanding and supersonic, but sonic just at the front: the CJ-equilibrium condition is a consequence of the Taylor-Zel'dovich-Döring (TZD) simple-wave solution $\eta(x/t)$ to the homentropic flow (uniform s) behind this constant-velocity planar front: $u + c = x/t \Rightarrow (u + c)_{\text{CJ}} = x_{\text{CJ}}/t \equiv D_{\text{CJ}}$, with t the time and x the position in the flow [39], [40], [14]. In contrast to a subsonic discontinuity ($u + c > D$), an acoustic perturbation in the flow or from the piston cannot reach the CJ front: $x < x_{\text{CJ}} \Rightarrow x/t = u + c < x_{\text{CJ}}/t = (u + c)_{\text{CJ}} = D_{\text{CJ}}$. This defines the CJ self-sustained detonation (App.B). The CJ velocity and state are then the functions $D_{\text{CJ}}(v_0, p_0)$ and $\eta_{\text{CJ}}(v_0, p_0)$ (15) of the only initial state, for example (17) and (91) (App.A).

20. If u_p is exactly set to u_{CJ} , the flow is both constant-state and CJ sonic: $u + c = x/t = (u + c)_{\text{CJ}} = x_{\text{CJ}}/t = D_{\text{CJ}}$. The velocity D is still equal to $D_{\text{CJ}}(v_0, p_0)$, which can therefore be interpreted as the smallest value reachable in a series of experiments carried out with constant values of u_p greater than, but closer and closer to $u_{\text{CJ}}(v_0, p_0)$ from one experiment to the other. Equivalently, this is the limiting flow after an infinite run distance of a CJ self-sustained detonation from ignition at a fixed wall ($u_p = 0$): the slopes of the $\eta(x/t)$ profiles at fixed position x tend to zero as t tends to infinity.

21. Therefore, an overdriven detonation can have the same velocity D with any initial state (v_0, p_0) if u_p is set to the proper value $u_p(v_0, p_0) \geq u_{\text{CJ}}(v_0, p_0)$ that ensures $D(u_p; v_0, p_0) = \text{const.}$; but there is no reason then why one of the final-state variables should also be invariant. Consequently, initial states must be selected specifically so that u_p can achieve invariances of both D and one final-state variable, which in this work is specific entropy s . For the sonic CJ detonation, the same initial states turn out to ensure that both s_{CJ} and D_{CJ} are constant: the invariances of D_{CJ} and s_{CJ} are equivalent constraints. Specific entropy s enters the problem only through the differentials of equations of state (1-a) and (2-b): the initial-variations problem for constant s and D has to be formulated as $ds = 0$ and $dD = 0$, which entails differentiating the Rankine-Hugoniot relations (6).

3.2 Rankine-Hugoniot differentials

22. The differentials of the Rayleigh-Michelson line (8-a), the Hugoniot relation (8-b) and the $h(p, v)$ equation of state (1-b) form the 3×3 non-homogeneous linear system for dv , dp and dh

$$\frac{v_0 dp}{D^2} + \frac{dv}{v_0} = 2 \left(1 - \frac{v}{v_0}\right) \frac{dD}{D} + \frac{v_0 dp_0}{D^2} - \left(1 - 2\frac{v}{v_0}\right) \frac{dv_0}{v_0}, \quad (20)$$

$$2\frac{dh}{D^2} - \left(1 + \frac{v}{v_0}\right) \frac{v_0 dp}{D^2} - \left(1 - \frac{v}{v_0}\right) \frac{dv}{v_0} = - \left(1 + \frac{v}{v_0}\right) \frac{v_0 dp_0}{D^2} + \left(1 - \frac{v}{v_0}\right) \frac{dv_0}{v_0} + 2\frac{dh_0}{D^2}, \quad (21)$$

$$\frac{dh}{D^2} - \frac{G+1}{G} \frac{v}{v_0} \frac{v_0 dp}{D^2} - \frac{M^{-2}}{G} \frac{v}{v_0} \frac{dv}{v_0} = 0, \quad (22)$$

which thus write as linear combinations of dD , dv_0 , dp_0 and $dh_0(p_0, v_0)$, for example,

$$(M^{-2} - 1) \frac{dv}{v_0} = - \left(1 - \frac{v}{v_0}\right) F \frac{dD}{D} + \left(1 - F \frac{v}{v_0}\right) \frac{dv_0}{v_0} - \frac{1 + (1-F) \frac{v}{v_0}}{1 - \frac{v}{v_0}} \frac{v_0 dp_0}{D^2} + \frac{2-F}{1 - \frac{v}{v_0}} \frac{dh_0}{D^2}, \quad (23)$$

$$\begin{aligned} (M^{-2} - 1) \frac{v_0 dp}{D^2} &= \left(1 - \frac{v}{v_0}\right) (F + 2(M^{-2} - 1)) \frac{dD}{D} - \left(1 - F \frac{v}{v_0} + (M^{-2} - 1) \left(1 - 2\frac{v}{v_0}\right)\right) \frac{dv_0}{v_0} \dots \\ &\dots + \frac{1 + (1-F) \frac{v}{v_0} + (M^{-2} - 1) \left(1 - \frac{v}{v_0}\right)}{1 - \frac{v}{v_0}} \frac{v_0 dp_0}{D^2} - \frac{2-F}{1 - \frac{v}{v_0}} \frac{dh_0}{D^2}. \end{aligned} \quad (24)$$

The differential ds of the specific entropy,

$$\frac{T ds}{D^2} = \left(1 - \frac{v}{v_0}\right)^2 \frac{dD}{D} + \left(1 - \frac{v}{v_0}\right) \frac{v}{v_0} \frac{dv_0}{v_0} - \frac{v}{v_0} \frac{v_0 dp_0}{D^2} + \frac{dh_0}{D^2}, \quad (25)$$

is obtained by substituting $dh(s, p)$ (1-a) for dh in (21) and by eliminating $v_0 dp/D^2 + dv/v_0$ with (20). The coefficients in (23) and (24) involve the three state functions v , $F(G, v)$ (11-b) and M : $dh(p, v)$ introduces the two state functions G and $c = (v/v_0)(D/M)$, from (6-a) and (9-b), and v , p and h are one-variable functions, from (7). In contrast, $dh(s, p)$ does not involve c , M and F , so neither does ds .

23. The determinant of system (20)-(22) is $M^{-2} - 1$, and the right-hand sides of (23) and (24) must be set to zero for CJ discontinuities ($M = 1$) so dv and dp can be finite. This defines the CJ velocity and entropy differentials dD_{CJ} and ds_{CJ} , from (25), as the eigenconstraints

$$F_{CJ} \frac{dD_{CJ}}{D_{CJ}} = \frac{1 - 2\frac{v_{CJ}}{v_0} + G_{CJ} \left(1 - \frac{v_{CJ}}{v_0} + \frac{v_0}{v_{CJ}} \frac{M_{0CJ}^{-2}}{G_0}\right)}{1 - \frac{v_{CJ}}{v_0}} \frac{dv_0}{v_0} - \frac{1 - G_{CJ} \frac{v_0}{v_{CJ}} \left(1 - \frac{v_{CJ}}{v_0} + \frac{1}{G_0}\right)}{1 - \frac{v_{CJ}}{v_0}} \frac{v_0 dp_0}{D_{CJ}^2}, \quad (26)$$

$$F_{CJ} \frac{T_{CJ} ds_{CJ}}{D_{CJ}^2} = \left(1 - \frac{v_{CJ}}{v_0} + \frac{2M_{0CJ}^{-2}}{G_0}\right) \frac{dv_0}{v_0} + \left(1 - \frac{v_{CJ}}{v_0} + \frac{2}{G_0}\right) \frac{v_0 dp_0}{D_{CJ}^2}, \quad (27)$$

after substituting $dh_0(p_0, v_0)$ for dh_0 . They can be directly obtained from (20), (21) and $dh(s, p)$, instead of $dh(p, v)$, by using the CJ condition $M = 1$ as $c/v = D/v_0$ (6-a) in $ds(p, v)$ (2-b) and then eliminating the combination $(v_0 dp_{CJ}/D_{CJ}^2) + (dv_{CJ}/v_0) = G_{CJ} (v_0/v_{CJ}) (T_{CJ} ds_{CJ}/D_{CJ}^2)$ [4], [42]. The derivation above provides the intermediate differentials (23) and (24) necessary to demonstrate the DSI theorem. Differentials (26) and (27) show that $F_{CJ} \neq 0$ (11-b) is also a necessary continuity condition: initial-state perturbations have to produce small variations of D_{CJ} and s_{CJ} (Subsect.2.2, App.B). In the acoustic limit ($D \rightarrow c_0$, $v/v_0 \rightarrow 1$, $F \rightarrow 2$), (25) and (27) coherently reduce to $dh_0(s_0, p_0)$.

24. The theorem demonstration is easier from a simpler writing of these differentials that introduces a distribution of p_0 and v_0 on an arbitrary polar curve $p_0^*(v_0)$ through a reference point $v_{0*}, p_{0*} = p_0^*(v_{0*})$. The initial enthalpy $h_0(p_0, v_0)$ reduces to the function $h_0^*(v_0) = h_0(p_0^*(v_0), v_0)$ of v_0 , hence, from (1-b),

$$\frac{v_0}{D^2} \frac{dh_0^*}{dv_0} = \frac{G_0 + 1}{G_0} \left(\frac{v_0}{D}\right)^2 \frac{dp_0^*}{dv_0} + \frac{M_0^{-2}}{G_0}. \quad (28)$$

The final-state expressions $\eta(D; v_0, p_0)$ (7) reduce to functions $\eta^*(D, v_0) = \eta(D; v_0, p_0^*(v_0))$ of D and v_0 , hence, from (23) and (25),

$$(M^{-2} - 1) \frac{dv^*}{v_0} = -F \left(1 - \frac{v}{v_0}\right) \frac{dD}{D} + \Phi_v^* \frac{dv_0}{v_0}, \quad (29)$$

$$\frac{T ds^*}{D^2} = \left(1 - \frac{v}{v_0}\right)^2 \frac{dD}{D} + \Phi_s^* \frac{dv_0}{v_0}, \quad (30)$$

where

$$\Phi_v^* = 1 - 2\frac{v}{v_0} + G\frac{v_0}{v} \left(\left(1 - \frac{v}{v_0}\right) \frac{v}{v_0} + \frac{M_0^{-2}}{G_0} \right) - \left(1 - G\frac{v_0}{v} \left(1 - \frac{v}{v_0} + \frac{1}{G_0}\right)\right) \left(\frac{v_0}{D}\right)^2 \frac{dp_0^*}{dv_0}. \quad (31)$$

$$\Phi_s^* = \left(1 - \frac{v}{v_0}\right) \frac{v}{v_0} + \frac{M_0^{-2}}{G_0} + \left(1 - \frac{v}{v_0} + \frac{1}{G_0}\right) \left(\frac{v_0}{D}\right)^2 \frac{dp_0^*}{dv_0}, \quad (32)$$

Similarly to $h_0(p_0, v_0)$, the CJ velocity $D_{CJ}(v_0, p_0)$ and specific entropy $s_{CJ}(v_0, p_0)$ reduce to the functions $D_{CJ}^*(v_0) = D_{CJ}(v_0, p_0^*(v_0))$ and $s_{CJ}^*(v_0) = s_{CJ}(v_0, p_0^*(v_0))$ of v_0 , hence, from (26) and (27),

$$\frac{v_0}{D_{CJ}} \frac{dD_{CJ}^*}{dv_0} = F_{CJ}^{-1} \left(1 - \frac{v_{CJ}}{v_0}\right)^{-1} \Phi_{v_{CJ}}^*, \quad (33)$$

$$\frac{v_0 T_{CJ}}{D_{CJ}^2} \frac{ds_{CJ}^*}{dv_0} = F_{CJ}^{-1} \left(1 - \frac{v_{CJ}}{v_0}\right) \Phi_{v_{CJ}}^* + \Phi_{s_{CJ}}^*. \quad (34)$$

25. The slope dp_0^*/dv_0 is thus the parameter that defines how the initial, final and CJ properties vary with v_0 for initial states varying on $p_0^*(v_0)$ (Fig.1). Final states varying at constant initial state lie on the same Hugoniot, initial states varying on $p_0^*(v_0)$ generate a $(p-v)$ arc of final states between a point U on a Hugoniot H with pole $O(v_0, p_0)$ and a point U' on another Hugoniot H' with pole $O'(v_0 + dv_0, p_0 + dp_0^*(v_0))$. The partial derivative $\partial\eta^*/\partial D)_{v_0}$ is the variation of η with respect to D along the same Hugoniot, $\partial\eta^*/\partial v_0)_D$ is the variation of η with respect to v_0 from one Hugoniot to another for piston speeds u_p (Subsect.3.1) chosen for each initial state on $p_0^*(v_0)$ so that the final states have the same D , and $\partial D/\partial v_0)_{s^*}$ and $\partial\eta^*/\partial v_0)_{s^*}$ are variations with respect to v_0 for u_p such that the final states are on the same isentrope arc. The demonstration requires that the partial derivative of v^* with respect to v_0 be finite along an equilibrium isentrope: physical CJ velocities are finite, so are isentrope slopes at CJ points (Subsect.3.4).

3.3 Demonstration and interpretation

26. Differentials (30) and (29) define two constraints on partial derivatives of $s^*(D, v_0)$ and $v^*(D, v_0)$

$$\Phi_s^* \equiv \left(\frac{v_0 T}{D^2} \frac{\partial s^*}{\partial v_0} \right)_D = - \left(1 - \frac{v}{v_0} \right)^2 \frac{v_0}{D} \frac{\partial D}{\partial v_0} \Big|_{s^*}, \quad (35)$$

$$\Phi_v^* \equiv (M^{-2} - 1) \frac{\partial v^*}{\partial v_0} \Big|_D = (M^{-2} - 1) \frac{\partial v^*}{\partial v_0} \Big|_{s^*} + F \left(1 - \frac{v}{v_0} \right) \frac{v_0}{D} \frac{\partial D}{\partial v_0} \Big|_{s^*}. \quad (36)$$

The first indicates that, regardless of M ,

$$\Phi_s^* \propto \left(\frac{\partial s^*}{\partial v_0} \right)_D = 0 \Leftrightarrow \left(\frac{\partial D}{\partial v_0} \right)_{s^*} = 0, \quad (37)$$

a consequence of the triple product rule, (30) being a two-variables differential,

$$\left(\frac{\partial s^*}{\partial v_0} \right)_D = - \left(\frac{\partial s^*}{\partial D} \right)_{v_0} \frac{\partial D}{\partial v_0} \Big|_{s^*} \quad \because \quad ds^* = \left(\frac{\partial s^*}{\partial D} \right)_{v_0} dD + \left(\frac{\partial s^*}{\partial v_0} \right)_D dv_0, \quad (38)$$

and $\partial s^*/\partial D \Big|_{v_0} = \left(1 - \frac{v}{v_0} \right)^2 (D^2/T) \neq 0$ (14-a). Neither of equality in (37) is true in general (Subsect.3.1) but both are so for sonic final states ($M = 1$): (36) and (37) give, successively,

$$\Phi_v^{*(M=1)} \propto \left(\frac{\partial D}{\partial v_0} \right)_{s^*}^{(M=1)} = 0, \quad \Phi_s^{*(M=1)} \propto \left(\frac{\partial s^*}{\partial v_0} \right)_D^{(M=1)} = 0 \quad (39)$$

if $\partial v^*/\partial v_0 \Big|_D^{(M=1)}$ and $\partial v^*/\partial v_0 \Big|_{s^*}^{(M=1)}$ are finite, hence the DSI theorem (19) from (33)-(34) or (38-b),

$$(ds^*)^{(M=1)} \equiv ds_{CJ}^* = 0 \Leftrightarrow (dD)^{(M=1)} \equiv dD_{CJ}^* = 0. \quad (40)$$

27. Equivalently, combining $dv^*(s, v_0)$ and (13-b), or (35) and (36), gives

$$\left(\frac{\partial v^*}{\partial v_0} \right)_D = \left(\frac{\partial v^*}{\partial v_0} \right)_s + \frac{\partial v^*}{\partial s} \Big|_{v_0} \frac{\partial s^*}{\partial v_0} \Big|_D \Leftrightarrow \Phi_s^* = (M^{-2} - 1) \left(1 - \frac{v}{v_0} \right) \left(\frac{\partial v^*}{\partial v_0} \right)_s - \frac{\partial v^*}{\partial v_0} \Big|_D \Big) F^{-1}, \quad (41)$$

so $\Phi_s^{*(M=1)} = 0$ if $(\partial v^*/\partial v_0)_s - \partial v^*/\partial v_0 \Big|_D^{(M=1)}$ is finite, then $\partial D/\partial v_0 \Big|_{s^*}^{(M=1)} = 0$ from (37), and $\Phi_v^{*(M=1)} = 0$ from (36). An initial state varied so that a CJ detonation retains the same velocity thus generates a CJ state that retains the same entropy. This can also be obtained from dp : the coefficients in (23) and (24) have same absolute values if $M = 1$. A model problem is proposed in Appendix C.

28. An interpretation in the p - v plane (Fig.1) considers the Hugoniot curves $p_H(v; p_0, v_0)$ (8-b) as a one-parameter family $y_H^*(p, v; v_0) = 0$ with parameter v_0 if their poles (p_0, v_0) are distributed on $p_0^*(v_0)$,

$$y_H^*(p, v; v_0) = -h(p, v) + h_0(p_0, v_0) + \frac{1}{2}(p - p_0)(v_0 + v), \quad p_0 = p_0^*(v_0). \quad (42)$$

This family has an envelope if $p_0^*(v_0)$ satisfies the constraint obtained by setting to zero the partial derivative of $y_H^*(p, v; v_0)$ with respect to v_0

$$\left(\frac{\partial y_H^*}{\partial v_0} \right)_{p,v} = 0 \Leftrightarrow \frac{dp_0^*}{dv_0} = - \left(\frac{D}{v_0} \right)^2 \times \frac{1 - \frac{v}{v_0} + \frac{2M_0^{-2}}{G_0}}{1 - \frac{v}{v_0} + \frac{2}{G_0}}. \quad (43)$$

This envelope is an isentrope if it is made up of sonic points, as the CJ-entropy differential (27) shows.

29. Similarly, the Rayleigh-Michelson lines (R) $p_R(v, D; p_0, v_0)$ (8-a) form a two-parameters family $y_R^*(p, v; D, v_0) = 0$, with parameters v_0 and D , if their poles (p_0, v_0) are distributed on $p_0^*(v_0)$,

$$y_R^*(p, v; D, v_0) = -p + p_0 + \left(\frac{D}{v_0}\right)^2 (v_0 - v), \quad p_0 = p_0^*(v_0). \quad (44)$$

which reduces to a one-parameter sub-family, with v_0 the only parameter, if D is a function of v_0 and p_0 such as D_{CJ} (15-a). Thus, with $D_{CJ}^*(v_0) = D_{CJ}(v_0, p_0^*(v_0))$, setting to zero the partial derivative of $y_R^*(p, v; D_{CJ}^*(v_0), v_0)$ with respect to v_0 gives the envelope constraint for the R lines

$$\frac{\partial y_R^*}{\partial v_0} = 0 \quad \Leftrightarrow \quad \frac{dp_0^*}{dv_0} = - \left(\frac{D_{CJ}^*}{v_0}\right)^2 \times \left(2 \frac{v_{CJ}}{v_0} - 1 + 2 \left(1 - \frac{v_{CJ}}{v_0}\right) \frac{v_0}{D_{CJ}^*} \frac{dD_{CJ}^*}{dv_0}\right), \quad (45)$$

which is an isentrope if it is made up of sonic points. This can be observed from

$$G \frac{v_0}{v} \frac{T ds_R}{D^2} = \frac{v_0 dp_0}{D^2} + \left(2 \frac{v}{v_0} - 1\right) \frac{dv_0}{v_0} + 2 \left(1 - \frac{v}{v_0}\right) \frac{dD}{D} + (M^{-2} - 1) \frac{dv}{v_0}, \quad (46)$$

obtained by combining the differentials of the R relation (20) and the $s(p, v)$ equation of state (2-b). The DSI theorem $dD_{CJ}^* = 0$ along an isentrope then gives

$$\frac{dp_0^*}{dv_0} = - \left(\frac{D_{CJ}^*}{v_0}\right)^2 \times \left(2 \frac{v}{v_0} - 1\right). \quad (47)$$

30. An isentrope is thus the common envelope (Fig.1) of families of equilibrium Hugoniots and Rayleigh-Michelson lines with initial states such that CJ detonations have the same velocity. The connection with Davis' implementation of the Inverse Method for condensed explosives [41] is discussed in Subsection 3.4.

3.4 Chapman-Jouguet supplemental properties

31. The initial-state variations dp_0 and dv_0 that ensure the invariances of D_{CJ} and s_{CJ} are the non-zero solutions to either 2×2 homogeneous systems $\{dD_{CJ} = 0 - ds_{CJ} = 0\}$ (26)-(27) or $\{\Phi_v^* = 0 - \Phi_s^* = 0\}_{CJ}$ (39-ab): their determinants are proportional to each other because any of their 4 constraints is a linear combination of the other 3. Setting either to zero, or identifying the envelope constraints (43) and (47) to each other, gives the condition

$$G_0 x_{CJ}^2 + 2x_{CJ} - (1 - M_{0CJ}^{-2}) = 0, \quad (48)$$

$$x_{CJ} = 1 - \frac{v_{CJ}}{v_0} = \frac{v_0 (p_{CJ} - p_0)}{D_{CJ}^2} = \frac{u_{CJ}}{D_{CJ}}. \quad (49)$$

The compressive solution $v_{CJ}/v_0 < 1$, $p_{CJ}/p_0 > 1$ and (17) form the one-variable (D_{CJ}) representation (18) of the CJ detonation state

$$v_{CJ}(D_{CJ}; v_0, p_0) = v_0 \frac{1 + G_0 - \sqrt{1 + G_0 (1 - M_{0CJ}^{-2})}}{G_0}, \quad (50)$$

$$p_{CJ}(D_{CJ}; v_0, p_0) = p_0 + \frac{D_{CJ}^2}{v_0} \frac{\sqrt{1 + G_0 (1 - M_{0CJ}^{-2})} - 1}{G_0}, \quad (51)$$

$$\gamma_{CJ}(D_{CJ}; v_0, p_0) = \frac{1 + G_0 - \sqrt{1 + G_0 (1 - M_{0CJ}^{-2})}}{G_0 \frac{p_0 v_0}{c_0^2} M_{0CJ}^{-2} - 1 + \sqrt{1 + G_0 (1 - M_{0CJ}^{-2})}}. \quad (52)$$

Conversely, D_{CJ} is a function of one CJ variable, for example, p_{CJ} with (51) or γ_{CJ} with (52):

$$\left(\frac{D_{\text{CJ}}}{c_0}\right)^2 = \pi_{\text{CJ}} \left(1 + \frac{1}{2\pi_{\text{CJ}}}\right) \left(1 + \sqrt{1 + \frac{G_0}{\left(1 + \frac{1}{2\pi_{\text{CJ}}}\right)^2}}\right), \text{ where } \pi_{\text{CJ}} = \frac{v_0(p_{\text{CJ}} - p_0)}{c_0^2}, \text{ and} \quad (53)$$

$$\left(\frac{D_{\text{CJ}}}{c_0}\right)^2 = \frac{(\gamma_{\text{CJ}} + 1)^2}{\gamma_{\text{CJ}}^2 - 1 - G_0} \left(\frac{1}{2} - \frac{1 + \frac{G_0}{\gamma_{\text{CJ}} + 1}}{\gamma_{\text{CJ}} + 1} \frac{\gamma_{\text{CJ}}}{\tilde{\gamma}_0} + \frac{1}{2} \sqrt{1 - \frac{4\left(1 + \frac{G_0 - (1 + G_0)\gamma_{\text{CJ}}}{\gamma_{\text{CJ}} + 1} \frac{\gamma_{\text{CJ}}}{\tilde{\gamma}_0}\right)}{\gamma_{\text{CJ}} + 1} \frac{\gamma_{\text{CJ}}}{\tilde{\gamma}_0}}\right), \quad (54)$$

where $\tilde{\gamma}_0 = c_0^2/p_0 v_0$ and must not be confused with γ_0 , except for gases (Subsect.2.1). Relation (54) shows a large sensitivity of D_{CJ} to γ_{CJ} , as is more evident in the gas example (56-b) below. The identity

$$G_0 = \frac{\alpha_0 c_0^2}{C_{p0}}, \quad \alpha_0 = \frac{1}{v_0} \left.\frac{\partial v_0}{\partial T_0}\right)_{p_0}, \quad (55)$$

indicates that the necessary initial data are c_0 , C_{p0} , and v_0 measured as a function of T_0 at constant p_0 so that the coefficient of thermal expansion α_0 can be determined.

32. For ideal gases, c , C_p , α and γ are functions of $T = pv(W/R)$ only, $G = \gamma - 1$, $v = RT/pW$, $\alpha = 1/T$. Thus, for initially-ideal gases,

$$\gamma_{\text{CJ}}(D_{\text{CJ}}, p_0, T_0) = \sqrt{\frac{\gamma_0}{1 - \frac{\gamma_0 - 1}{\gamma_0} M_{0\text{CJ}}^{-2}}}, \quad D_{\text{CJ}}^2(\gamma_{\text{CJ}}, p_0, T_0) = \frac{1 - \gamma_0^{-1}}{1 - \frac{\gamma_0}{\gamma_{\text{CJ}}}} \times c_0^2, \quad (56)$$

$$\frac{D_{\text{CJ}}^2(p_{\text{CJ}}, p_0, T_0)}{v_0 p_{\text{CJ}}} = \left(1 - \left(1 - \frac{\gamma_0}{2}\right) \frac{p_0}{p_{\text{CJ}}}\right) \left(1 + \sqrt{1 + \frac{(\gamma_0 - 1) \left(1 - \frac{p_0}{p_{\text{CJ}}}\right)^2}{\left(1 - \left(1 - \frac{\gamma_0}{2}\right) \frac{p_0}{p_{\text{CJ}}}\right)^2}}\right). \quad (57)$$

The strong-shock limits ($M_{0\text{CJ}}^{-2} \ll 1$ or $p_0/p_{\text{CJ}} \ll 1$) of γ_{CJ} and D_{CJ}^2 are $\sqrt{\gamma_0}$ and $(1 + \sqrt{\gamma_0}) v_0 p_{\text{CJ}}$, respectively (their acoustic limits are γ_0 and c_0^2). The typical values $\gamma_0 = 1.3$, $c_0 = 330$ m/s and $D_{\text{CJ}} = 2000$ m/s give $\gamma_{\text{CJ}} = 1.144$, $\sqrt{\gamma_0} = 1.140$ and relative error $100 \times (\gamma_{\text{CJ}}/\sqrt{\gamma_0} - 1) = 0.316$ %. Relations (56) and (57) apply to initially-ideal gases, but products may be non-ideal if p_0 is large enough.

33. The (p_0, v_0) pairs that achieve invariance of D_{CJ} or s_{CJ} are solutions to the ordinary differential equation formed by substituting (50) for v in (43) or (47). The initial condition is a reference initial state (p_{0*}, v_{0*}) with known CJ velocity D_{CJ}^* . The particular solution is the polar curve $p_0^*(v_0)$ through (p_{0*}, v_{0*}) , which, substituted for p_0 in $v_{\text{CJ}}(D_{\text{CJ}}; v_0, p_0)$ (50) and $p_{\text{R}}(v, D; v_0, p_0)$ (8-a) gives

$$v_{\text{CJ}}^*(v_0) = v_{\text{CJ}}(v_0, p_0^*(v_0), D_{\text{CJ}}^*), \quad p_{\text{CJ}}^*(v_0) = p_0^*(v_0) + \frac{D_{\text{CJ}}^{*2}}{v_0} \left(1 - \frac{v_{\text{CJ}}^*(v_0)}{v_0}\right). \quad (58)$$

The isentrope $p_{\text{S}}^*(v)$ is generated by eliminating v_0 between $v_{\text{CJ}}^*(v_0)$ and $p_{\text{CJ}}^*(v_0)$, that is, by varying v_0 and representing $p_{\text{CJ}}^*(v_0)$ as a function of $v_{\text{CJ}}^*(v_0)$. Thus, v_0 can parameterize an isentrope of detonation products. This, however, necessitates C_{p0} , c_0 and v_0 in a sufficiently large (p_0, T_0) domain whereas calculating the CJ state from (50), (51) and (52) necessitates them for one initial state only.

34. Physically, the DSI theorem holds because isentrope have finite slopes, so the derivatives $\partial z^*/\partial v_0)_s$ and $\partial z^*/\partial v_0)_D$ are finite and non-zero at sonic points (Subsect.3.3). Formally, this is obtained by differentiating $c(s, v)$ (3-b) and the mass balance (6-a) written as $v = v_0 M(c/D)$,

$$\frac{dv}{v} = \frac{dv_0}{v_0} + \frac{dc}{c} + \frac{dM}{M} - \frac{dD}{D}, \quad (59)$$

$$dc = \left.\frac{\partial c}{\partial s}\right)_v ds + \left.\frac{\partial c}{\partial v}\right)_s dv, \quad (60)$$

hence, restricting variations to an isentrope,

$$\Gamma \left(\frac{v_0}{v} \frac{\partial v}{\partial v_0} \right)_s = 1 - \left(\frac{v_0}{D} \frac{\partial D}{\partial v_0} \right)_s + \left(\frac{v_0}{M} \frac{\partial M}{\partial v_0} \right)_s, \quad (61)$$

with Γ the fundamental derivative of hydrodynamics (5). The sonic condition $M = \text{const.} = 1$ and the DSI consequence $\partial D / \partial v_0 \Big|_{s^*}^{(M=1)} = 0$ (39-a), combined with (4), (1-a) and (6-a), then give

$$\left(\frac{\partial v^*}{\partial v_0} \right)_{s^*}^{(M=1)} = - \left(\frac{v_0}{D_{\text{CJ}}} \right)^2 \left(\frac{\partial p^*}{\partial v_0} \right)_{s^*}^{(M=1)} = \Gamma_{\text{CJ}}^{-1} \frac{v_{\text{CJ}}}{v_0}, \quad (62)$$

$$\frac{v_0}{D_{\text{CJ}}^2} \left(\frac{\partial h^*}{\partial v_0} \right)_{s^*}^{(M=1)} = -\Gamma_{\text{CJ}}^{-1} \left(\frac{v_{\text{CJ}}}{v_0} \right)^2, \quad \frac{v_0}{D_{\text{CJ}}} \left(\frac{\partial u^*}{\partial v_0} \right)_{s^*}^{(M=1)} = (1 - \Gamma_{\text{CJ}}^{-1}) \frac{v_{\text{CJ}}}{v_0}. \quad (63)$$

Therefore, the derivatives of v , p and h are finite and non-zero at a CJ point except if $\Gamma_{\text{CJ}} \rightarrow \infty$ and $\Gamma_{\text{CJ}} = 0$, respectively (the derivative of u is zero for $\Gamma_{\text{CJ}} = 1$), and the constraints $\partial v^* / \partial v_0 \Big|_{s^*}^{(M=1)} < \infty$ and $\partial v^* / \partial v_0 \Big|_D^{(M=1)} < \infty$ are equivalent to each other. In contrast, with z denoting v , p or h , the derivatives $\partial z^* / \partial D \Big|_{v_0}^{(M=1)}$ are infinite (or $\partial D / \partial z^* \Big|_{v_0}^{(M=1)} = 0$), as (14-b) shows. In the perfect-gas example (App.A), taking the partial derivative of $v(D; v_0, p_0)$ (96) with respect to D moves the square-root term at the denominator, so $\lim_{D \rightarrow D_{\text{CJ}}} \partial v / \partial D \Big|_{p_0, v_0} = -\infty$, whereas its partial derivative with respect to v_0 , with $p_0 = p_0^*(v_0)$, shows that $\lim_{D \rightarrow D_{\text{CJ}}} \partial v^* / \partial v_0 \Big|_D$ is finite if $\partial D / \partial v_0 \Big|_{s^*} = 0$.

35. The ratio $dD_{\text{CJ}}/ds_{\text{CJ}}$ is obtained by eliminating dp_0/dv_0 between (26) and (27). The non-homogenous term is zero from 48), hence

$$\frac{D_{\text{CJ}} dD_{\text{CJ}}}{T_{\text{CJ}} ds_{\text{CJ}}} = \left(1 - \frac{v_{\text{CJ}}}{v_0} \right)^{-2} \left(1 - F_{\text{CJ}} \frac{1 + G_0 \left(1 - \frac{v_{\text{CJ}}}{v_0} \right)}{2 + G_0 \left(1 - \frac{v_{\text{CJ}}}{v_0} \right)} \right). \quad (64)$$

36. The partial derivatives of $D_{\text{CJ}}(v_0, p_0)$, and those of $D_{\text{CJ}}(T_0, p_0)$, are not independent since there are initial-state variations for which D_{CJ} is constant. This is implied by the triple product rule,

$$\left(\frac{\partial D_{\text{CJ}}}{\partial z_0} \right)_{p_0} = - \left(\frac{\partial p_0}{\partial z_0} \right)_{D_{\text{CJ}}} \left(\frac{\partial D_{\text{CJ}}}{\partial p_0} \right)_{z_0}, \quad (65)$$

where z_0 denotes either v_0 or T_0 . Hence, with $\partial p_0 / \partial v_0 \Big|_{D_{\text{CJ}}}$ given by (43) or (47),

$$\frac{v_0}{D_{\text{CJ}}} \left(\frac{\partial D_{\text{CJ}}}{\partial v_0} \right)_{p_0} = \left(2 \frac{v_{\text{CJ}}}{v_0} - 1 \right) \frac{D_{\text{CJ}}}{v_0} \left(\frac{\partial D_{\text{CJ}}}{\partial p_0} \right)_{v_0}, \quad (66)$$

$$\frac{D_{\text{CJ}}}{v_0} \left(\frac{\partial D_{\text{CJ}}}{\partial p_0} \right)_{T_0} = \frac{1 - (1 + \alpha_0 T_0 G_0) \left(2 \frac{v_{\text{CJ}}}{v_0} - 1 \right) M_{0\text{CJ}}^2 T_0}{\left(2 \frac{v_{\text{CJ}}}{v_0} - 1 \right) \alpha_0 T_0} \frac{T_0}{D_{\text{CJ}}} \left(\frac{\partial D_{\text{CJ}}}{\partial T_0} \right)_{p_0}, \quad (67)$$

the latter being obtained from the former and the identities

$$\frac{T_0}{D_{\text{CJ}}} \left(\frac{\partial D_{\text{CJ}}}{\partial T_0} \right)_{p_0} = \alpha_0 T_0 \frac{v_0}{D_{\text{CJ}}} \left(\frac{\partial D_{\text{CJ}}}{\partial v_0} \right)_{p_0}, \quad (68)$$

$$\frac{D_{\text{CJ}}}{v_0} \left(\frac{\partial D_{\text{CJ}}}{\partial p_0} \right)_{T_0} = \frac{v_0}{D_{\text{CJ}}} \left(\frac{\partial D_{\text{CJ}}}{\partial p_0} \right)_{v_0} - M_0^2 (1 + \alpha_0 T_0 G_0) \frac{v_0}{D_{\text{CJ}}} \left(\frac{\partial D_{\text{CJ}}}{\partial v_0} \right)_{p_0}. \quad (69)$$

The variations of D_{CJ} with respect to T_0 at constant p_0 thus determine those with respect to p_0 at constant T_0 , and conversely. The 5 constraints above also apply to s_{CJ} since $\partial p_0 / \partial z_0 \Big|_{D_{\text{CJ}}} = \partial p_0 / \partial z_0 \Big|_{s_{\text{CJ}}}$.

37. A reminder here on the Inverse Method (IM) (Sect.1, Subsect.3.2) is helpful to discuss below the DSI theorem and its application to liquid explosives in Subsection 4.2. Manson [4] and Wood and Fickett [42] were the first to discuss several IM implementations depending on the pair of independent initial-state variables. For liquids, the two options used in this work are more conveniently introduced from

$$\frac{dD_{CJ}}{D_{CJ}} = \frac{1 - F_{CJ}(1 - x_{CJ})}{F_{CJ}x_{CJ}} \frac{dv_0}{v_0} - \frac{1 + (1 - F_{CJ})(1 - x_{CJ})}{F_{CJ}x_{CJ}^2} \frac{v_0 dp_0}{D_{CJ}^2} + \frac{2 - F_{CJ}}{F_{CJ}x_{CJ}^2} \frac{dh_0}{D_{CJ}^2} \quad (70)$$

obtained by setting $M = 1$ in dv (23) or dp (24), and with x_{CJ} given by (49). The first option considers the same homogeneous explosive, and thus either pair (v_0, p_0) or (T_0, p_0) subject to $v_0(T_0, p_0)$ and $h_0(p_0, v_0)$ (1-b) or $h_0(T_0, p_0)$ (2-a): the pair (v_0, p_0) first reduces (70) to (26), measurement of $D_{CJ}(v_0, p_0)$ would next give values of $\partial D_{CJ}/\partial v_0|_{p_0}$ and $\partial D_{CJ}/\partial p_0|_{v_0}$, and their identification to their expressions in (26) then gives, after elimination of F_{CJ} or G_{CJ} (11-b), the CJ state from the solution $x_{CJ} < 1$ of

$$G_0 L x_{CJ}^2 + 2K x_{CJ} - (1 - M_{0CJ}^{-2}) = 0, \quad (71)$$

with L and K for $D_{CJ}(v_0, p_0)$ and $D_{CJ}(T_0, p_0)$ given by

$$\begin{aligned} L &= 1 + \left. \frac{D_{CJ}}{v_0} \frac{\partial D_{CJ}}{\partial p_0} \right)_{v_0} - \left. \frac{v_0}{D_{CJ}} \frac{\partial D_{CJ}}{\partial v_0} \right)_{p_0} \\ &= 1 + \left. \frac{D_{CJ}}{v_0} \frac{\partial D_{CJ}}{\partial p_0} \right)_{T_0} + \left. \frac{1 - M_{0CJ}^{-2} + \alpha_0 T_0 G_0}{\alpha_0 T_0 M_{0CJ}^{-2}} \frac{T_0}{D_{CJ}} \frac{\partial D_{CJ}}{\partial T_0} \right)_{p_0}, \end{aligned} \quad (72)$$

$$\begin{aligned} K &= 1 + M_{0CJ}^{-2} \left. \frac{D_{CJ}}{v_0} \frac{\partial D_{CJ}}{\partial p_0} \right)_{v_0} - \left. \frac{v_0}{D_{CJ}} \frac{\partial D_{CJ}}{\partial v_0} \right)_{p_0} \\ &= 1 + M_{0CJ}^{-2} \left. \frac{D_{CJ}}{v_0} \frac{\partial D_{CJ}}{\partial p_0} \right)_{T_0} + \left. \frac{G_0 T_0}{D_{CJ}} \frac{\partial D_{CJ}}{\partial T_0} \right)_{p_0}. \end{aligned} \quad (73)$$

Substituting (66) for $\partial D_{CJ}/\partial p_0|_{v_0}$, or (67) for $\partial D_{CJ}/\partial p_0|_{T_0}$, in (71), coherently returns (48), that is, the CJ state depends on D_{CJ} only, and not on its derivatives for initial-state variations that satisfy (43) or (47). The second option uses the pair (v_0, h_0) at constant p_0 . This can be achieved by means of a set of isometric mixtures [43], that is, with the same atomic composition, and thus the same equilibrium equation of state, for any value of the composition parameter, denoted below by w_0 [42]. This amounts to determining $h_0(T_0, w_0)$ and $v_0(T_0, w_0)$ and measuring $D_{CJ}(T_0, w_0)$ at constant p_0 . Setting $dp_0 = 0$ in (70) first gives the differential of $D_{CJ}(v_0, h_0)$, measurement of $D_{CJ}(v_0, h_0)$ at constant p_0 would next give values of $\partial D_{CJ}/\partial v_0|_{h_0, p_0}$ and $\partial D_{CJ}/\partial h_0|_{v_0, p_0}$, and their identification to their expressions in (70) then gives, after elimination of F_{CJ} , the CJ state from the solution $x_{CJ} < 1$ of

$$L x_{CJ}^2 + 2K x_{CJ} - 1 = 0, \quad (74)$$

where, with w_0 defined as the mass fraction of all components added to a reference explosive ($w_0 = 0$), L and K for $D_{CJ}(v_0, h_0)$ and $D_{CJ}(T_0, w_0)$ are given by

$$L = \left. D_{CJ} \frac{\partial D_{CJ}}{\partial h_0} \right)_{v_0, p_0} = \frac{\left. \frac{\omega_0 T_0}{D_{CJ}} \frac{\partial D_{CJ}}{\partial T_0} \right)_{w_0, p_0} - \left. \frac{\alpha_0 T_0}{D_{CJ}} \frac{\partial D_{CJ}}{\partial w_0} \right)_{T_0, p_0}}{\omega_0 \frac{C_{p0} T_0}{D_{CJ}^2} - \alpha_0 T_0 \Omega_0}, \quad (75)$$

$$K = 1 - \left. \frac{v_0}{D_{CJ}} \frac{\partial D_{CJ}}{\partial v_0} \right)_{h_0, p_0} = 1 + \frac{\left. \frac{\Omega_0 D_{CJ}}{T_0} \frac{\partial D_{CJ}}{\partial T_0} \right)_{w_0, p_0} - \left. \frac{C_{p0} T_0}{D_{CJ}^3} \frac{\partial D_{CJ}}{\partial w_0} \right)_{T_0, p_0}}{\omega_0 \frac{C_{p0} T_0}{D_{CJ}^2} - \alpha_0 T_0 \Omega_0}, \quad (76)$$

upon using the identities

$$\frac{dv_0}{v_0} = \alpha_0 T_0 \frac{dT_0}{T_0} + \omega_0 dw_0, \quad \omega_0 = \frac{1}{v_0} \left. \frac{\partial v_0}{\partial w_0} \right|_{T_0, p_0}, \quad (77)$$

$$\frac{dh_0}{D^2} = \frac{C_{p_0} T_0}{D^2} \frac{dT_0}{T_0} + \Omega_0 dw_0, \quad \Omega_0 = \frac{1}{D^2} \left. \frac{\partial h_0}{\partial w_0} \right|_{T_0, p_0}. \quad (78)$$

The denominator in L and K is the determinant of the $(v_0, h_0) - (T_0, w_0)$ mapping and is not zero, unless fortuitously. The CJ properties of the reference explosive are obtained by setting $w_0 = 0$ in (75)-(76). This second option is more convenient than the first because sufficiently-large variations of p_0 are uneasy to achieve and because it does not necessitate c_0 . However, contrary to the DSI theorem, both options assume independent partial derivatives of D_{CJ} , so the cumulation of their experimental uncertainties may limit the accuracy of their CJ predictions (Subsect.4.2). The IM also gives the CJ Gruneisen coefficient (3-a) as a function of two derivatives of D_{CJ} similarly to the CJ state, but the CJ supplemental properties give this coefficient only if one partial derivative of D_{CJ} is known.

38. The DSI method for obtaining an isentrope may appear similar to that in Davis' implementation of the IM [41] with the specific volume v_0 and energy e_0 as the independent variables, and p_0 neglected. Davis pointed out that particular v_0 and e_0 can be poles of Hugoniot that have an isentrope as an envelope, which he then calculated from a given function $D_{CJ}(e_0, v_0)$. The constraint $ds = 0$ can indeed be satisfied with other independent variables than p_0 and v_0 since the Hugoniot relation (8-b) involves only state variables: using h_0 and v_0 as the independent variables at constant p_0 , the same reasonings as in Subsection 3.3 to demonstrate and interpret the DSI theorem shows that an isentrope is an envelope to a family of Hugoniot for subsets $h_0^*(v_0)$ that satisfy

$$\frac{dh_0^*}{dv_0} = -\frac{1}{2} (p - p_0), \quad (79)$$

and that, from (45), the envelope condition for a family of Rayleigh-Michelson lines is

$$\frac{v_0}{D} \frac{dD}{dv_0} = \frac{1}{2} \frac{1 - 2\frac{v}{v_0}}{1 - \frac{v}{v_0}} \equiv 1 - \left(2 \frac{v_0 (p - p_0)}{D^2} \right)^{-1}. \quad (80)$$

These 2 relations reduce to Davis' eqs.(31)and (14), respectively, using (17) and neglecting p_0/p . However, evidently enough, the joint invariance of s_{CJ} and D_{CJ} here implies that v_{CJ}/v_0 is constant and equal to 1/2, that is, $\gamma_{CJ} = 1$: the DSI theorem, $dD_{CJ} = 0 \Leftrightarrow ds_{CJ} = 0$, can be physically satisfied only if p_0 is varied, even if the non-dimensional values p_0/p or $v_0 p_0 / D^2$ are negligibly small.

39. No pair of CJ variables other than D_{CJ} and s_{CJ} can be non-trivially invariant, that is, with non-zero dp_0 and dv_0 : the differentials of the Rankine-Hugoniot relations and the equations of state subject to the invariance of a pair of final-state variables produce a 2×2 homogeneous linear system for dp_0 and dv_0 (with dh_0 subject to (22)), but only the D_{CJ} - s_{CJ} invariant pair produces a non-trivially null determinant; relation (48) is this annulment condition. For example, in the $p - v$ plane, no non-zero dp_0 and dv_0 permit a focal point $dp_{CJ} = 0 - dv_{CJ} = 0$: since $s = s(p, v)$ and $h = h(p, v)$, this would imply $ds_{CJ} = 0$ and $dh_{CJ} = 0$, and, from (20), $dD_{CJ} = 0$, which represents the Rayleigh-Michelson line through p_0, v_0 .

40. The DSI theorem, and the IM, are valid only for initial and equilibrium states described with two-variables equations of state. The differentiations in this analysis thus consistently include equilibrium shifts (Subsect.2.1): there is no reason for different initial states to generate the same frozen final composition. Finally, it should be noted that the DSI theorem ensures but does not imply these properties.

4. Application to gaseous or liquid explosives

41. Entropy of detonation products cannot be measured. As for gaseous explosives (Subsect.4.1), the DSI theorem and some CJ supplemental properties were thus analysed by means of chemical equilibrium calculations. Only ideal detonation products were investigated so as to avoid the uncertainties induced by equations of state, such as those of condensed explosives, calibrated from experiments that may not have achieved the strict CJ equilibrium (Sect.1). The calculations were done with the NASA computer program CEA [38]. As for liquid explosives (Subsect.4.2), the analysis is a comparative discussion of the theoretical CJ pressures from (51) and values from experiments and the Inverse Method (Subsect.3.4).

4.1 Gaseous explosives with ideal final states

42. Tables 1 show numerical values of s_{CJ} and D_{CJ} for the four stoichiometric mixtures $CH_4 + 2 O_2$, $C_3H_8 + 5 O_2$, $CH_4 + 2 \text{ Air}$ and $H_2 + 0.5 \text{ Air}$. Five (T_0, p_0) pairs with T_0 evenly spaced between 200 K and 400 K were used so as to represent a largest physical range. The third pair ($T_0 = 298.15$ K, $p_0 = 1$ bar) was chosen as the reference initial state (v_{0*}, p_{0*}) (subscript *, Subsect.3.3), and the p_0 values were determined by dichotomy for each T_0 so that the CJ entropies have the reference value s_{CJ}^* . The results were analysed based on the CJ-velocity mean values \bar{D}_{CJ} , absolute and mean relative deviations $\Delta D_{CJ}/\bar{D}_{CJ}$ and $m_{D_{CJ}}$, in percent, and corrected standard deviations $\sigma_{D_{CJ}}$

$$\bar{D}_{CJ} = \frac{1}{I} \sum_{i=1}^{I=5} D_{CJi}, \quad \left(\frac{\Delta D_{CJ}}{\bar{D}_{CJ}} \right)_i = 100 \times \frac{D_{CJi} - \bar{D}_{CJ}}{\bar{D}_{CJ}}, \quad (81)$$

$$m_{D_{CJ}} = \frac{1}{I} \sum_{i=1}^{I=5} \left| \frac{\Delta D_{CJ}}{\bar{D}_{CJ}} \right|_i, \quad \sigma_{D_{CJ}} = \sqrt{\frac{\sum_{i=1}^{I=5} (D_{CJi} - \bar{D}_{CJ})^2}{I-1}}. \quad (82)$$

All $m_{D_{CJ}}$'s and $\sigma_{D_{CJ}}$'s are very small. In particular, the D_{CJ} 's have the same mean values \bar{D}_{CJ} to $\mathcal{O}(0.1)$ % at most, and the agreement is practically exact for the $C_3H_8 + 5 O_2$ mixture. This suggests that an iterative minimization procedure of both $\Delta D_{CJ}/\bar{D}_{CJ}$ and $\Delta s_{CJ}/\bar{s}_{CJ}$ should return values of $p_0(T_0)$, \bar{D}_{CJ} and \bar{s}_{CJ} that even better satisfy the theorem and eliminate the slight decreasing trend of D_{CJ} with increasing T_0 at constant s_{CJ}^* observed here: the $p_0(T_0)$ values and the results in tables 1 can be seen as zeroth-order iterates. The $(v_0(T_0), p_0)$ pairs defined by the T_0 's and p_0 's in tables 1 therefore well approximate the polar curve $p_0^*(v_0)$ through (v_{0*}, p_{0*}) (Subsect.3.3). It is easy, albeit tedious, to check that another reference than $T_0^* = 298.15$ K and $p_0^* = 1$ bar returns similarly small $m_{D_{CJ}}$'s and $\sigma_{D_{CJ}}$'s.

43. These small values were validated by means of a sensitivity analysis based on initial states very close to a reference *, and CEA's numerical accuracy as a criterion. Table 2 shows results for the $C_3H_8 + 5 O_2$ mixture with three groups of four (T_0, p_0) pairs. The first pairs (bold) are the firsts, thirds and fifths in tables 1, so they generate the same entropy s_{CJ}^* ; their CJ states were used as references of their group (superscript *). The seconds (italics) have T_0 's only 5 % greater than in the firsts and p_0 's determined by dichotomy so that $s_{CJ} = s_{CJ}^*$; the $\Delta D_{CJ}/D_{CJ}^*$'s are thus at most equal to the $\mathcal{O}(10^{-2})$ % $m_{D_{CJ}}$'s in table 1-b, and smaller T_0 variations would be non-significant. The thirds and fourths are variations at constant T_0 and constant p_0 , respectively. In each group, the initial variations chosen to generate the same s_{CJ}^* (the seconds) give the smaller variations of T_{CJ} , which all are greater than CEA's $\mathcal{O}(10^{-3})$ % accuracy $\tilde{dT}/T = \tilde{dp}/p = 0.005$ % ([38], p.35, eqs.7.24, and p.40) by at least one order of magnitude. The initial variations chosen not to generate the same entropy s_{CJ}^* (the thirds and fourths) give variations of D_{CJ} 10 times greater than $m_{D_{CJ}}$ and the same $\mathcal{O}(10^{-1})$ % magnitude for those of s_{CJ} and T_{CJ} . Therefore, the small $\mathcal{O}(10^{-2})$ % variations of D_{CJ} at constant s_{CJ} , and the larger ones of s_{CJ} and D_{CJ} at constant T_0 and p_0 , are valid and not biases due to initial states chosen too close to each other. The variations

of s_{CJ} are slightly smaller than those of T_{CJ} : the combination of $dh(s, p)$ (1-a), $dh(T) = C_p dT$ (2-a), $pv = RT/W$ and $\gamma = C_p/C_v$, subject to $\tilde{d}T/T = \tilde{d}p/p$, gives

$$\frac{\tilde{d}s}{s} = (2 - \gamma^{-1}) \frac{C_p}{s} \times \frac{\tilde{d}T}{T} = \mathcal{O}(10^{-1} - 1) \times \frac{\tilde{d}T}{T}, \quad (83)$$

since typical γ , s and C_p are $\mathcal{O}(1)$, $\mathcal{O}(10)$ kJ/K/kg and $\mathcal{O}(1-10)$ kJ/K/kg, respectively. At $p_0 = 1$ bar and $T_0 = 298.15$ K, CEA gives $\tilde{d}s_{\text{CJ}}/s_{\text{CJ}} = 0.33 \times \tilde{d}T_{\text{CJ}}/T_{\text{CJ}}$ for $CH_4 + 2$ Air, and $\tilde{d}s_{\text{CJ}}/s_{\text{CJ}} = 0.89 \times \tilde{d}T_{\text{CJ}}/T_{\text{CJ}}$ for $CH_4 + 2$ O_2 .

44. The theoretical (theo) ratios $r_{\text{CJ}} = (\rho_{\text{CJ}}/\rho_0, p_{\text{CJ}}/p_0, \gamma_{\text{CJ}})$ were calculated from (17) and (56-a) using CEA values of D_{CJ} and the initial-state variables, and compared to CEA numerical (num) values. Tables 3 and 4 show initial data and results for C_3H_8/O_2 mixtures with equivalence ratios ER= 0.8, 1 and 2, $T_0 = 200$ K, 298.15 K and 400 K, and $p_0 = 0.2$ bar, 1 bar and 5 bar. Numbers are rounded, hence non-significant discrepancies between the indicated relative differences ϵ_r and those that can be calculated from rounded $r_{\text{CJ}}^{(\text{num})}$ and $r_{\text{CJ}}^{(\text{theo})}$,

$$\epsilon_r = 100 \times \frac{r_{\text{CJ}}^{(\text{num})} - r_{\text{CJ}}^{(\text{theo})}}{r_{\text{CJ}}^{(\text{num})}}. \quad (84)$$

All ϵ_r 's are small, ranging from $\mathcal{O}(10^{-1})$ to $\mathcal{O}(1)$ %, but greater than the $\mathcal{O}(10^{-2} - 10^{-1})$ % $m_{D_{\text{CJ}}}$'s, likely because of the sensitivity to the initial thermodynamic coefficients: the accuracy of C_{p0} determines the others. The uncertainties of s_{CJ} , γ_{CJ} , ρ_{CJ} and p_{CJ} are obtained from $ds(p, v)$ (1-b), (17-a-b), $pv = RT/W$, $\gamma_{\text{CJ}}^2 \approx \gamma_0 = C_{p0}/C_{v0}$ (56-a) and $C_{p0} - C_{v0} = R/W_0$; the typical values $M_{0\text{CJ}}^{-2} \ll 1$, $\gamma_{\text{CJ}}^2 \approx \gamma_0 \approx G_{\text{CJ}} + 1 \approx 1.2$, $s_{\text{CJ}} \approx 10^4$ J/kg, $R \approx 8$ J/kg/mole, $W_{\text{CJ}} \approx 2 \times 10^{-2}$ kg/mole, and the Newtonian limit $\gamma_{\text{CJ}} \approx 1^+$, then give the estimates

$$\frac{\delta s_{\text{CJ}}}{s_{\text{CJ}}} = \frac{2}{s_{\text{CJ}} G_{\text{CJ}}} \frac{R}{W} \frac{1 - M_{0\text{CJ}}^{-2}}{1 + M_{0\text{CJ}}^{-2}/\gamma_0} \frac{\delta D_{\text{CJ}}}{D_{\text{CJ}}} \approx \frac{1}{10} \frac{\delta D_{\text{CJ}}}{D_{\text{CJ}}}, \quad (85)$$

$$\frac{\delta \gamma_{\text{CJ}}}{\gamma_{\text{CJ}}} = \frac{1}{2} \left(1 + \frac{M_{0\text{CJ}}^{-2}/\gamma_0}{1 - \frac{\gamma_0 - 1}{\gamma_0} M_{0\text{CJ}}^{-2}} \right) \frac{\delta \gamma_0}{\gamma_0} + \frac{\frac{\gamma_0 - 1}{\gamma_0} M_{0\text{CJ}}^{-2}}{1 - \frac{\gamma_0 - 1}{\gamma_0} M_{0\text{CJ}}^{-2}} \frac{\delta D_{\text{CJ}}}{D_{\text{CJ}}} \approx \frac{1}{2} \frac{\delta \gamma_0}{\gamma_0} = \frac{\delta C_{p0}}{C_{p0}}, \quad (86)$$

$$\frac{\delta \rho_{\text{CJ}}}{\rho_{\text{CJ}}} = \frac{-1}{\gamma_{\text{CJ}} + 1} \frac{\delta \gamma_{\text{CJ}}}{\gamma_{\text{CJ}}} + \frac{2M_{0\text{CJ}}^{-2}/\gamma_0}{1 + M_{0\text{CJ}}^{-2}/\gamma_0} \frac{\delta D_{\text{CJ}}}{D_{\text{CJ}}} \approx \frac{-1}{4} \frac{\delta \gamma_0}{\gamma_0} = \frac{-1}{2} \frac{\delta C_{p0}}{C_{p0}}, \quad (87)$$

$$\frac{\delta p_{\text{CJ}}}{p_{\text{CJ}}} = \frac{-\gamma_{\text{CJ}}}{\gamma_{\text{CJ}} + 1} \frac{\delta \gamma_{\text{CJ}}}{\gamma_{\text{CJ}}} + \frac{2}{1 + M_{0\text{CJ}}^{-2}/\gamma_0} \frac{\delta D_{\text{CJ}}}{D_{\text{CJ}}} \approx \frac{-1}{4} \frac{\delta \gamma_0}{\gamma_0} = \frac{-1}{2} \frac{\delta C_{p0}}{C_{p0}}. \quad (88)$$

The first shows that D_{CJ} is 10 times more sensitive than s_{CJ} , which validates the choice above of analysing the DSI theorem with initial states generating the same s_{CJ} rather than the same D_{CJ} . The next three show that γ_{CJ} is twice more sensitive than ρ_{CJ} and p_{CJ} , with p_{CJ} slightly more so than ρ_{CJ} (table 4). The same is true for other mixtures: $\epsilon_\gamma = -3.4$ % whereas $m_{D_{\text{CJ}}} = 0.08$ % for $CH_4 + 2$ O_2 at $T_0 = 298.15$ K and $p_0 = 1$ bar. The uncertainty of γ_{CJ} is twice as small as that of γ_0 , and thus the same as that of C_{p0} . The magnitude of $\delta C_{p0}/C_{p0}$ depends T_0 , p_0 and on the mixture components and proportions; a sensitivity study to thermochemical databases should be carried out.

45. These calculations support physically and numerically the DSI theorem in a large range of initial conditions: the larger $\Delta D_{\text{CJ}}/\bar{D}_{\text{CJ}}$'s at constant s_{CJ} are very small, smaller than at constant p_0 or T_0 , and not numerical uncertainties. They also support the CJ supplemental properties: their differences with the numerical ones is very small and smaller than the physical uncertainty of thermochemical coefficients. The same trends were obtained with the five fuels CH_4 , C_2H_2 , C_2H_4 , C_2H_6 and H_2 .

TABLES 1. Joint invariances of CJ entropy s_{CJ} and velocity D_{CJ} : CJ-velocity mean value \bar{D}_{CJ} , absolute relative deviation $\Delta D_{CJ}/\bar{D}_{CJ}$, mean relative deviation $m_{D_{CJ}}$, and corrected standard deviation $\sigma_{D_{CJ}}$ of 4 mixtures.

$CH_4 + 2 O_2$ $m_{D_{CJ}} = 0.08 \%$ $\bar{D}_{CJ} = 2389.7$ m/s $\sigma_{D_{CJ}} = 2.47$ m/s					$C_3H_8 + 5 O_2$ $m_{D_{CJ}} = 0.012 \%$ $\bar{D}_{CJ} = 2356.7$ m/s $\sigma_{D_{CJ}} = 0.41$ m/s				
T_0 (K)	p_0 (bar)	s_{CJ} (kJ/kg/K)	D_{CJ} (m/s)	$\frac{\Delta D_{CJ}}{\bar{D}_{CJ}}$ (%)	T_0 (K)	p_0 (bar)	s_{CJ} (kJ/kg/K)	D_{CJ} (m/s)	$\frac{\Delta D_{CJ}}{\bar{D}_{CJ}}$ (%)
200.00	0.6284	id*	2392.9	0.13	200.00	0.6304	id*	2357.3	0.03
250.00	0.8118	id*	2391.2	0.06	250.00	0.8127	id*	2356.7	~ 0.00
298.15*	1.0000*	12.6653*	2389.6	~ 0.00	298.15*	1.0000*	11.9293*	2356.3	-0.01 ₅
350.00	1.2165	id*	2388.0	-0.07	350.00	1.2165	id*	2356.3	-0.01 ₅
400.00	1.4410	id*	2386.7	-0.12	400.00	1.4419	id*	2356.7	~ 0.00
$CH_4 + 2$ Air $m_{D_{CJ}} = 0.05 \%$ $\bar{D}_{CJ} = 1799.9$ m/s $\sigma_{D_{CJ}} = 1.23$ m/s					$H_2 + 0.5$ Air $m_{D_{CJ}} = 0.1 \%$ $\bar{D}_{CJ} = 1964.7$ m/s $\sigma_{D_{CJ}} = 2.55$ m/s				
T_0 (K)	p_0 (bar)	s_{CJ} (kJ/kg/K)	D_{CJ} (m/s)	$\frac{\Delta D_{CJ}}{\bar{D}_{CJ}}$ (%)	T_0 (K)	p_0 (bar)	s_{CJ} (kJ/kg/K)	D_{CJ} (m/s)	$\frac{\Delta D_{CJ}}{\bar{D}_{CJ}}$ (%)
200.00	0.6044	id*	1801.4	0.08	200.00	0.6004	id*	1967.9	0.16
250.00	0.7968	id*	1800.7	0.05	250.00	0.7941	id*	1966.4	0.08
298.15*	1.0000*	9.4218*	1799.9	~ 0.00	298.15*	1.0000*	10.5927*	1964.8	~ 0.00
350.00	1.2401	id*	1799.1	-0.04	350.00	1.2444	id*	1963.1	-0.08
400.00	1.4949	id*	1798.3	-0.09	400.00	1.5042	id*	1961.5	-0.16

TABLE 2. Joint invariances of CJ entropy s_{CJ} and velocity D_{CJ} : sensitivity to small changes of initial state of the $C_3H_8+5 O_2$ mixture.

T_0 (K)	p_0 (bar)	s_{CJ} (kJ/kg/K)	$\frac{\Delta s_{CJ}}{s_{CJ}^*}$ (%)	D_{CJ} (m/s)	$\frac{\Delta D_{CJ}}{\bar{D}_{CJ}^*}$ (%)	T_{CJ} (K)	$\frac{\Delta T_{CJ}}{T_{CJ}^*}$ (%)
200.00*	0.6304*	11.9293*	/	2357.3*	/	3799.46*	/
210.00	0.6660	11.9293*	/	2357.1	-0.01	3801.57	0.06
200.00	0.6660	11.9093	-0.17	2359.7	0.10	3810.15	0.28
210.00	0.6304	11.9493	0.17	2354.7	-0.14	3790.91	-0.22
298.15*	1.0000*	11.9293*	/	2356.3*	/	3821.11*	/
313.06	1.0606	11.9293*	/	2356.3	0.00	3824.64	0.09
298.15	1.0606	11.9078	-0.18	2358.9	0.11	3832.68	0.30
313.06	1.0000	11.9508	0.18	2353.6	-0.11	3813.09	-0.21
400.00*	1.4419*	11.9293*	/	2356.7*	/	3846.74*	/
420.00	1.5371	11.9293*	/	2356.9	0.01	3852.19	0.14
400.00	1.5371	11.9059	-0.20	2359.6	0.12	3859.48	0.33
420.00	1.4419	11.9527	0.20	2354.0	-0.11	3839.46	-0.19

TABLE 3. Initial data for calculating the theoretical CJ state from the CJ velocity D_{CJ} for C_3H_8/O_2 mixtures with 3 equivalence ratios ER and 3 initial temperatures T_0 and pressures p_0 (table 4, theo).

C_3H_8/O_2	T_0 (K)	p_0 (bar)	ER = 0.8	ER = 1	ER = 1.2	
W_0 (g/mol)			33.667	34.015	34.340	
γ_0	200.		1.3390	1.3286	1.3194	
	298.15		1.3061	1.2924	1.2807	
	400.		1.2716	1.2563	1.2434	
c_0 (m/s)	200.		257.2	254.9	252.8	
	298.15		310.1	306.9	304.1	
	400.		354.4	350.5	347.0	
v_0 (m ³ /kg)	200.	0.2	2.4696	2.4444	2.4212	
		1	0.4939	0.4889	0.4842	
		5	0.0988	0.0978	0.0968	
	298.15	0.2	3.6816	3.6439	3.6094	
		1	0.7363	0.7288	0.7219	
		5	0.1473	0.1458	0.1444	
	400.	0.2	4.9393	4.8887	4.8425	
		1	0.9878	0.9777	0.9685	
		5	0.1976	0.1956	0.1937	
	D_{CJ} (m/s)	200.	0.2	2203.9	2306.7	2392.0
			1	2269.8	2377.6	2466.1
			5	2334.7	2447.5	2538.8
298.15		0.2	2182.5	2284.6	2369.8	
		1	2249.2	2356.3	2444.7	
		5	2315.4	2427.6	2518.9	
400.		0.2	2165.5	2267.6	2352.9	
		1	2233.2	2340.1	2428.6	
		5	2300.6	2412.6	2504.2	

TABLE 4. Comparison of numerical (num) and theoretical (theo) CJ properties (r_{CJ}) for C_3H_8/O_2 mixtures with 3 equivalence ratios ER and 3 initial temperatures T_0 and pressures p_0 .

T_0 (K)	p_0 (bar)	r_{CJ}	ER = 0.8			ER = 1			ER = 1.2		
			num	theo	ϵ_r (%)	num	theo	ϵ_r (%)	num	theo	ϵ_r (%)
200.	0.2	ρ_{CJ}/ρ_0	1.870	1.844	<i>1.38</i>	1.870	1.849	<i>1.14</i>	1.870	1.854	<i>0.86</i>
		p_{CJ}/p_0	46.746	46.010	<i>1.58</i>	51.635	50.966	<i>1.29</i>	55.950	55.402	<i>0.98</i>
		γ_{CJ}	1.125	1.159	<i>-3.03</i>	1.127	1.154	<i>-2.41</i>	1.130	1.150	<i>-1.81</i>
	1	ρ_{CJ}/ρ_0	1.864	1.845	<i>1.02</i>	1.865	1.850	<i>0.77</i>	1.863	1.855	<i>0.47</i>
		p_{CJ}/p_0	49.354	48.775	<i>1.17</i>	54.602	54.121	<i>0.88</i>	59.180	58.861	<i>0.54</i>
		γ_{CJ}	1.134	1.159	<i>-2.23</i>	1.136	1.154	<i>-1.60</i>	1.139	1.150	<i>-0.96</i>
	5	ρ_{CJ}/ρ_0	1.859	1.846	<i>0.69</i>	1.859	1.851	<i>0.43</i>	1.858	1.856	<i>0.11</i>
		p_{CJ}/p_0	51.990	51.580	<i>0.79</i>	57.612	57.325	<i>0.50</i>	62.436	62.357	<i>0.13</i>
		γ_{CJ}	1.142	1.159	<i>-1.50</i>	1.144	1.154	<i>-0.86</i>	1.148	1.150	<i>-0.19</i>
298.15	0.2	ρ_{CJ}/ρ_0	1.861	1.844	<i>0.92</i>	1.863	1.852	<i>0.58</i>	1.863	1.858	<i>0.27</i>
		p_{CJ}/p_0	30.939	30.617	<i>1.04</i>	34.170	33.947	<i>0.65</i>	37.031	36.919	<i>0.30</i>
		γ_{CJ}	1.123	1.146	<i>-1.98</i>	1.125	1.139	<i>-1.23</i>	1.128	1.134	<i>-0.53</i>
	1	ρ_{CJ}/ρ_0	1.856	1.846	<i>0.55</i>	1.857	1.854	<i>0.20</i>	1.857	1.860	<i>-0.12</i>
		p_{CJ}/p_0	32.696	32.491	<i>0.63</i>	36.165	36.084	<i>0.23</i>	39.206	39.262	<i>-0.14</i>
		γ_{CJ}	1.132	1.145	<i>-1.18</i>	1.134	1.139	<i>-0.43</i>	1.137	1.134	<i>0.32</i>
	5	ρ_{CJ}/ρ_0	1.852	1.848	<i>0.20</i>	1.852	1.855	<i>-0.16</i>	1.852	1.861	<i>-0.50</i>
		p_{CJ}/p_0	34.486	34.406	<i>0.23</i>	38.204	38.273	<i>-0.18</i>	41.418	41.654	<i>-0.57</i>
		γ_{CJ}	1.140	1.145	<i>-0.43</i>	1.143	1.139	<i>0.34</i>	1.146	1.133	<i>1.11</i>
400.	0.2	ρ_{CJ}/ρ_0	1.852	1.845	<i>0.38</i>	1.855	1.855	<i>-0.00</i>	1.855	1.862	<i>-0.39</i>
		p_{CJ}/p_0	22.843	22.747	<i>0.42</i>	25.232	25.233	<i>-0.00</i>	27.352	27.471	<i>-0.43</i>
		γ_{CJ}	1.122	1.131	<i>-0.79</i>	1.124	1.124	<i>-0.04</i>	1.126	1.117	<i>0.79</i>
	1	ρ_{CJ}/ρ_0	1.848	1.848	<i>-0.01</i>	1.850	1.857	<i>-0.39</i>	1.850	1.864	<i>-0.78</i>
		p_{CJ}/p_0	24.162	24.164	<i>-0.01</i>	26.726	26.843	<i>-0.44</i>	28.982	29.238	<i>-0.88</i>
		γ_{CJ}	1.131	1.131	<i>-0.01</i>	1.133	1.123	<i>0.85</i>	1.136	1.117	<i>1.63</i>
	5	ρ_{CJ}/ρ_0	1.843	1.850	<i>-0.36</i>	1.845	1.859	<i>-0.76</i>	1.845	1.866	<i>-1.17</i>
		p_{CJ}/p_0	25.512	25.618	<i>-0.41</i>	28.262	28.505	<i>-0.86</i>	30.652	31.059	<i>-1.33</i>
		γ_{CJ}	1.139	1.131	<i>0.77</i>	1.142	1.123	<i>1.62</i>	1.145	1.117	<i>2.43</i>

4.2 Liquid explosives

46. Four liquids were investigated, namely nitromethane (NM, CH_3NO_2), isopropyl nitrate (IPN, $C_3H_7NO_3$), hot trinitrotoluene (TNT, $C_7H_5N_3O_6$) and niprona (NPNA3, $C_3H_{10}N_4O_{11}$), a stoichiometric compound made up of 1 volume of 2-nitropropane ($C_3H_7NO_2$) and 3 volumes of nitric acid (HNO_3). Table 5 compares their theoretical CJ detonation pressures (theo), calculated from (51) and experimental detonation velocities, to values obtained from the Inverse Method (IM, Subsect.3.4) and experiments (exp). Tables 6 and 7 show the sensitivity of the IM results for NM and IPN; those in table 5 were obtained with the most probable $D_{CJ}^{(exp)}$ derivatives (Tabs.6 and 7, second lines and columns). The results bring out very contrasted trends. Essentially, all theoretical pressures are significantly greater than the experimental and the IM pressures except IPN's (Tab.5); but they may actually agree with the IM pressures because of the uncertainties of the initial data and the velocity derivatives (Tabs.6 and 7-right). The adiabatic exponents γ were calculated from (51-b), so their low theoretical values are consistent with the large ones of the theoretical pressures. The analysis below is an unsuccessful and speculative disentanglement of uncertainties and physics.

47. The data are ancient but reliable, and still referred to, e.g. [44] and [45] for IPN. In liquids, however, the initial properties can vary slowly over time, and so can the detonation properties, which also depend on chemical and physical purities, such as diethylenetriamine or micro-bubbles. No reference here ensures that measurements were carried out with the same batches of explosives over short enough periods. For NM, four data sets — *I*, *II*, *III*, *IV* — at $T_0 = 4$ C and $p_0 = 1$ bar were thus retained so as to assess the sensitivity of the calculations. For NM *I*, they are those in Brochet and Fisson [46] and, for NM *II*, those in Davis, Craig and Ramsay [47], except for c_0 , which is that in [46]. For NM *III*, the initial properties are those in Lysne and Hardesty [48], except for C_{p0} , calculated with the fit $C_{p0}(J/kg/K) = 1720.9 + 0.54724 \times T_0(C)$ of Jones and Giauque's measurements [49] between the melting (245 K) and ambient (298 K) temperatures; the CJ properties are those in [46]. For NM *IV*, ρ_0 and α_0 are calculated with the fit $\rho_0(kg/m^3) = 1152.0 - 1.1395 \times T_0(C) - 1.665 \times 10^{-3} \times T_0^2(C)$ in Berman and West [50]. For IPN, the data are those in [46], for NPNA3, those in Bernard, Brossard, Claude and Manson [51] and, for TNT, those in [47] and [52], except for c_0 , identified to the constant a of the linear asymptote $D = a + bu$ to Garn's shock Hugoniot measurements [53]. The derivatives of $D_{CJ}^{(exp)}$ necessary to implement the IM (Subsect.3.4) could be found only for NM and IPN. They are those of $D_{CJ}^{(exp)}(T_0, p_0)$ in [46] for NM and IPN (Tabs.6 and 7-right), and those of $D_{CJ}^{(exp)}(T_0, w_0)$ in [47] for NM (Tab.7-left) from isometric mixtures of NM and mass fractions w_0 of acenina, a compound made up of equal volumes of methyl cyanide (CH_3CN), nitric acid (HNO_3) and water (H_2O), so its atomic composition is proportionally identical to that of NM (CH_3NO_2).

48. For NM, the theoretical pressures (51) are insensitive to the initial uncertainties (Tab.5) but not the (T_0, p_0) -IM pressures (Tab.6) which can even agree with the former: the same value $p_{CJ} = 17.9$ GPa is obtained with $\rho_0 = 1149$ kg/m³ and $\alpha_0 = 1.023$ K⁻¹, comprised between those for NM *III* and *IV*, and with $\partial D_{CJ}^{(exp)}/\partial T_0 = -3.96$ m/s/K and $\partial D_{CJ}^{(exp)}/\partial p_0 = 0.191 \times 10^{-5}$ m/s/bar, comprised in the uncertainty intervals of these derivatives. In contrast, the (T_0, w_0) -IM pressures (Tab.7-left) are insensitive to initial uncertainties (results not shown for concision). The differences thus more likely result from the measurements of the detonation properties or the physical assumptions of this analysis.

49. The measured detonation properties are only assumed to be CJ-equilibrium. The velocities $D_{CJ}^{(exp)}$ are linear extrapolations to infinite diameters of values measured in finite-diameter tubes. The question is how large their diameters should be so that D_{CJ} is not underestimated or the propagation regime is not sonic-frozen, perhaps even low-velocity. There are many analyses of the diameter effect in condensed explosives (Sect.1). The recent one by Chiquete and Short [54] indicates that characteristics originating from the explosive-tube interface may intersect the frozen sonic surface on its side opposite to the curved leading shock. The CJ-equilibrium detonation, or equivalently the TZD self-similar equilibrium expansion

(Subsect.3.1) at the end of the ZND steady planar reaction zone, thus seems to be a hydrodynamic limit difficult to reach in a stick of condensed explosive: the flow is always diverging at the cylinder edge. This is supported by Sharpe’s numerical simulations [6] of ignition by an overdriven detonation with a one-step reversible reaction rate in the long-time limit: a stable reaction zone relaxes to the CJ-equilibrium state for the planar wave, but to sonic frozen states for the spherically-diverging wave, even at large radii. Pressure measurements, for example by flyer-impact or Doppler-velocimetry techniques, cannot be adequately discussed here, but at least it should be reminded that a slope discontinuity on an experimental profile is not necessarily a CJ-equilibrium locus and that extracting such a discontinuity from the signal noise can be difficult. The theory of hyperbolic equations, such as Euler’s balance equations for inviscid fluids, ensures that it is a sonic front, but it is more likely frozen, similarly to that in the diameter effect. The latter would only be marginally involved here: the theoretical pressures calculated from experimental velocities are greater than measurements. Detonation tubes at least should be as wide and long as possible, but the longer they are, the smaller the jump of derivatives of the TZD and the ZND flows at the sonic locus, and so the more difficult is its detection: the TZD derivatives tend towards zero with increasing detonation run distance (Subsect.3.1), as do physical ZND derivatives with decreasing distance to the reaction-zone end.

50. Davis, Craig and Ramsay [47], [25] refuted the CJ-equilibrium hypothesis for condensed explosives because their (T_0, w_0) -IM implementation predicted lower pressures than experiments for NM and TNT. Their conclusion was criticized by Petrone [55] who considered that their interpretation of measurements overestimated the experimental pressures: for NM at 4 C (Tab.5), they retained 14.8 GPa instead of the usual values 12 – 14 GPa produced by most measurements and both the (T_0, p_0) - and (T_0, w_0) -IM implementations with their most probable velocity derivatives (Tab.6, excl. NM *IV*, and Tab.7-left). A point is that the (T_0, w_0) -IM pressures are smaller than the theoretical values and not very sensitive to the $D_{CJ}^{(exp)}(T_0, w_0)$ derivatives (Tab.7-left) (and to those of $v_0(w_0)$ and $h_0(w_0)$, Subsect.3.4, eqs.(77)-(78), results not shown for concision). However, the (T_0, p_0) -IM implementation for NM *III* also produces 14.8 GPa with velocity derivatives comprised in their uncertainty intervals (Tab.6), that is, $\partial D_{CJ}^{(exp)}/\partial T_0 = -4.12$ m/s/K and $\partial D_{CJ}^{(exp)}/\partial p_0 = 0.2 \times 10^{-5}$ m/s/bar. Similarly, the theoretical and the (T_0, p_0) -IM pressures can be equal to each other: for NM *III*, the theoretical value 17.4 GPa is obtained with the values of derivatives $\partial D_{CJ}^{(exp)}/\partial T_0 = -4.12$ m/s/K and $\partial D_{CJ}^{(exp)}/\partial p_0 = 0.1902 \times 10^{-5}$ m/s/bar, which are comprised in their uncertainty intervals and, importantly, satisfy their DSI compatibility relationship (67). An analytical analysis of sensitivity of the IM is possible but cumbersome and could not be developed here, and the velocity derivatives are not sufficiently numerous and accurate for soundly discussing the CJ hypothesis from IM pressures. Nevertheless, the theoretical CJ pressures are found not very sensitive to the initial data and greater than measurements and most IM estimates (Tab.5), with differences exceeding the fair experimental uncertainty ± 10 kbar.

51. Thus, at least one of the physical assumptions should be investigated. These include front adiabaticity, flow instabilities, single-phase fluid, local thermodynamic equilibrium, and sonic-frozen reaction end states (Sect.1). For example, NM, TNT and IPN have negative oxygen balances and thus large amounts of solid carbon in their detonation products. However, NPNA3 is stoichiometric and yet these four liquids all have theoretical CJ pressures greater than measurements: solid carbon aggregation is known as inherent to high-pressure chemical physics [17] p.186-190, [18], [19]. This questions the modelling of detonation products and reaction zones in carbonate liquids similarly to gases as single-phase fluids, such as in this work. The carbon agglomerates might have smaller speeds than the gas flow due to drag effects, and an endothermic aggregation might prevent achievement of the CJ equilibrium, and rather selects CJ-frozen states with pressures lower than the CJ-equilibrium value (Sect.1). A single material speed and a two-variables $T(p, v)$ equilibrium equation of state to fit measurements and predict CJ properties might not be valid assumptions for carbonate condensed explosives; multi-phase balance laws and constitutive relations with thermal and mechanical non-equilibria should be more systematically contemplated.

TABLE 5. Comparison of CJ detonation pressures and adiabatic exponents (exp: experiments, IM: Inverse Method (IM), theo: CJ supplemental properties) at $p_0 = 1$ bar for nitromethane (NM), isopropyl nitrate (IPN), niprona (NPNA3), and trinitrotoluene (TNT). Symbol \emptyset : no data.

	T_0 (C)	ρ_0 (kg/m ³)	$\alpha_0 \times 10^3$ (1/K)	C_{p0} (J/kg/K)	c_0 (m/s)	G_0	$D_{CJ}^{(exp)}$ (m/s)	p_{CJ} (GPa)			γ_{CJ}		
								exp	IM	theo	exp	IM	theo
<i>I</i>	4	1156	1.19	1747	1423	1.38	6330	12.7	12.9	17.5	2.65	2.58	1.65
NM <i>II</i>	4	1159	1.16	1733	1423	1.36	6334	14.8	12.6	17.6	2.14	2.69	1.65
<i>III</i>	4	1151	1.22	1723	1400	1.39	6330	12.7	13.6	17.4	2.63	2.39	1.65
<i>IV</i>	4	1147	1.00	1723	1400	1.14	6330	12.7	15.8	17.9	2.62	1.90	1.57
IPN	40	1017	1.23	1867	1049	0.72	5330	08.7	13.1	12.1	2.32	1.21	1.40
NPNA3	25	1275	1.11	1512	1184	1.03	6670	\emptyset	14.1	22.8	\emptyset	3.02	1.49
TNT	93	1450	0.70	1573	2140	2.04	6590	18.2	\emptyset	21.1	2.46	\emptyset	2.00

TABLE 6. Nitromethane (NM) at $T_0 = 277$ K and $p_0 = 1$ bar: sensitivity of the Inverse-Method pressures p_{CJ}^{IM} (in GPa) and adiabatic exponents γ_{CJ}^{IM} to the uncertainties of derivatives of measured detonation velocities $D_{CJ}^{(exp)}(T_0, p_0)$ and the initial data (table 5). Symbol /: no solution to (71).

$\partial D_{CJ}^{(exp)}/\partial p_0 \Big _{T_0}$		$\partial D_{CJ}^{(exp)}/\partial T_0 \Big _{p_0} \pm 0.18$ (m/s/K)											
± 0.01 (m/s/bar)		-4.14				-3.96				-3.78			
		<i>I</i>	<i>II</i>	<i>III</i>	<i>IV</i>	<i>I</i>	<i>II</i>	<i>III</i>	<i>IV</i>	<i>I</i>	<i>II</i>	<i>III</i>	<i>IV</i>
0.19	p_{CJ}^{IM}	16.1	16.5	17.8	/	14.4	14.7	15.4	19.0	13.2	13.4	13.9	16.1
	γ_{CJ}^{IM}	1.87	1.81	1.59	/	2.22	2.17	2.00	1.40	2.50	2.46	2.32	1.85
0.20	p_{CJ}^{IM}	14.0	14.3	15.0	18.5	12.9	13.2	13.6	15.8	12.1	12.3	12.6	14.3
	γ_{CJ}^{IM}	2.30	2.25	2.08	1.48	2.58	2.53	2.39	1.90	2.83	2.79	2.66	2.22
0.21	p_{CJ}^{IM}	12.7	12.9	13.3	15.5	11.9	12.1	12.4	14.0	11.3	11.4	11.6	13.0
	γ_{CJ}^{IM}	2.65	2.61	2.46	1.96	2.89	2.85	2.72	2.28	3.12	3.08	2.96	2.54

TABLES 7. Sensitivity of the Inverse-Method pressures p_{CJ}^{IM} (in GPa) and adiabatic exponents γ_{CJ}^{IM} to the uncertainties of derivatives of measured detonation velocities. **Left:** $D_{CJ}^{(exp)}(T_0, w_0)$ for nitromethane (NM *II*) at $T_0 = 277$ K and $p_0 = 1$ bar, acenina mass fraction $w_0 = 0$, $\partial h_0/\partial w_0 \Big|_{T_0, p_0} = (-2.021 \pm 0.17) \times 10^6$ (J/kg), $\partial v_0/\partial w_0 \Big|_{T_0, p_0} = (1.5 \pm 0.2) \times 10^{-3}$ (m³/kg). **Right:** $D_{CJ}^{(exp)}(T_0, p_0)$ for isopropyl nitrate (IPN) at $T_0 = 313$ K and $p_0 = 1$ bar. Symbol /: no solution to (71).

$\partial D_{CJ}^{2(exp)}/\partial w_0 \Big _{T_0, p_0}$		$\partial D_{CJ}^{(exp)}/\partial T_0 \Big _{w_0, p_0} \pm 0.18$ (m/s/K)			$\partial D_{CJ}^{(exp)}/\partial p_0 \Big _{T_0}$		$\partial D_{CJ}^{(exp)}/\partial T_0 \Big _{p_0} \pm 0.10$ (m/s/K)		
$\pm 0.18 \times 10^6$ (m ² /s ²)		-4.14	-3.96	-3.78	± 0.1 (m/s/bar)		-4.13	-4.03	-3.93
-8.16	p_{CJ}^{IM}	12.4	12.6	12.7	0.2	p_{CJ}^{IM}	/	/	/
	γ_{CJ}^{IM}	2.74	2.70	2.66		γ_{CJ}^{IM}	/	/	/
-7.98	p_{CJ}^{IM}	12.5	12.6	12.7	0.3	p_{CJ}^{IM}	15.9	13.1	11.8
	γ_{CJ}^{IM}	2.73	2.69	2.65		γ_{CJ}^{IM}	<i>i</i> 1	1.21	1.45
-7.80	p_{CJ}^{IM}	12.5	12.7	12.8	0.4	p_{CJ}^{IM}	7.3	7.2	7.0
	γ_{CJ}^{IM}	2.72	2.67	2.63		γ_{CJ}^{IM}	2.94	3.03	3.12

5. Discussion and conclusions

52. This work brought out two new features of the CJ-equilibrium model of detonation. The first one is that the CJ velocity and specific entropy are invariant under the same variations of the initial temperature and pressure (Subsect.3.3). The second one is essentially that no equation of state of detonation products is necessary to calculate simply the CJ state from the CJ velocity value, or the CJ velocity from one CJ variable (Subsect.3.4). They apply only if the initial and burnt states are single-phase fluids with temperature and pressure as the two independent state variables (Subsect.2.1). This is the case of ideal gases, for which detailed thermochemical calculations indeed validate these features very accurately (Subsect.4.1). However, the analysis of their overestimates of experimental pressures of four carbonate liquid explosives (Subsect.4.2) suggests further discussion on the assumptions of thermal and mechanical equilibria in their reaction zones and detonation products, and on whether their reaction processes can achieve the CJ chemical equilibrium (Sect.1). Inductively, this might apply to most carbonate condensed explosives to varying degrees, so initial and detonation data for a non-carbonate liquid explosive would benefit further investigations. Ammonium nitrate (NH_4NO_3) above its melting temperature (443 K) could apply but its metastability at elevated temperatures raises a safety issue.

53. Although not yet reported, they could have been obtained many years ago: they derive fairly simply from long-time known balance laws of basic hydrodynamics, namely the Rankine-Hugoniot relations contained in the single-phase adiabatic Euler equations. Their ubiquity today is the outcome of the prompting 40 years ago to develop numerical simulation of detonation dynamics. Thermal and mechanical non-equilibria at elevated pressures and temperatures have long been a theoretical and numerical challenge; averaged balance laws and constitutive relations built from various mixture rules are workarounds to fit in with this single-phase paradigm. The CJ supplemental properties of this work should be seen as go-betweens for experiments and models. In particular, they allow for a coherent discussion of this homogenization approach, but they are not substitutes for predictive thermochemical calculations. This justifies the question as to what if anything has been gained in comparison to the usual methodology of separate measurements of pressure and velocity for calibrating constitutive relations by means of numerical simulations: essentially, there is now a criterion, both experimental and numerical, to check simply if pressures are compatible with velocities as representative of the CJ-equilibrium state, and, if not, a basis for discussing the measurement conditions and the modelling assumptions.

54. The hyperbolic Euler equations combined with explicit equations of state form a closed set for which a data distribution on a non-characteristic side of a surface defines a well-posed Cauchy problem without using entropy. The sonic side of the CJ front is a particular case of characteristic distribution of data, and entropy was here a necessary intermediate to obtain these new features without equation of state for the fluid on this characteristic side: the velocity of the surface and the initial state give the characteristic state, or the initial state and one characteristic-state variable give the velocity of the surface. This might be inherent to hyperbolic systems and the wider group of characteristic horizons, such as surfaces of Schwarzschild black holes; the CJ-equilibrium detonation front is the horizon of events in the TZD expansion for an observer in the ZND reaction zone.

Appendix A. Chapman-Jouguet relations for the perfect gas

A.1. The perfect gas is the ideal gas with constant heat capacities $\bar{C}_v = (R/W)/(\bar{\gamma} - 1)$ and $\bar{C}_p = (R/W)\bar{\gamma}/(\bar{\gamma} - 1)$, with W the molecular weight and $R = 8.31451$ J/mol.K the gas constant. The adiabatic exponent γ is the constant ratio $\bar{\gamma} = \bar{C}_p/\bar{C}_v$, the Gruneisen coefficient G is $\bar{\gamma} - 1$, the fundamental derivative Γ is $(\bar{\gamma} + 1)/2$, and an isentrope writes $pv^{\bar{\gamma}} = \text{const}$. For the reactive perfect gas, the relation $T(p, v) = (W/R)pv$ reduces (2-a) to $dh(T) = C_p(T) dT$ whose integration gives the difference of enthalpies (89) of the products at (T, p) and the fresh gas at (T_0, p_0) (neglecting the differences of their W and $\bar{\gamma}$), which substituted for $h - h_0$ in (8-b) then gives the Hugoniot (90):

$$h(p, v) - h_0(p_0, v_0) = \frac{\bar{\gamma}(pv - p_0v_0)}{\bar{\gamma} - 1} - Q_0, \quad (89)$$

$$p_{\text{H}}(v; v_0, p_0) = p_0 \times \frac{1 - \frac{\bar{\gamma}-1}{\bar{\gamma}+1} \left(\frac{v}{v_0} - \frac{2Q_0}{p_0v_0} \right)}{\frac{v}{v_0} - \frac{\bar{\gamma}-1}{\bar{\gamma}+1}}. \quad (90)$$

A.2. A CJ state is given by (17) with $\bar{\gamma}$ substituted for γ_{CJ} , and a CJ velocity D_{CJ} is then a solution to the 2nd degree equation obtained by substituting p_{CJ} and v_{CJ} (17-ab) for p and v in (90). The supersonic compressive solution (subscript CJc, Subsect.2.3) is the velocity D_{CJc} of the CJ detonation

$$D_{\text{CJc}}(v_0, p_0) = \tilde{D}_{\text{CJ}} \left(\frac{1}{2} + \tilde{M}_{0\text{CJ}}^{-2} + \frac{1}{2} \sqrt{1 + 4\tilde{M}_{0\text{CJ}}^{-2}} \right)^{\frac{1}{2}}, \quad (91)$$

$$\tilde{D}_{\text{CJ}}^2 = 2(\bar{\gamma}^2 - 1)Q_0, \quad \tilde{M}_{0\text{CJ}} = \tilde{D}_{\text{CJ}}/c_0, \quad (92)$$

which has dominant value \tilde{D}_{CJ} if $\tilde{M}_{0\text{CJ}}^{-2} \ll 1$, and tends to c_0 in the non-reactive limit $Q_0 = 0$. The subsonic expansive solution (subscript CJx) is the velocity D_{CJx} of the CJ deflagration that is deduced from D_{CJc} by changing the sign before the square root in (91); they relate with each other by

$$D_{\text{CJc}}D_{\text{CJx}} = c_0^2 \quad \text{or} \quad M_{0\text{CJc}}M_{0\text{CJx}} = 1, \quad (93)$$

which had not been pointed out before. It shows that D_{CJx} has dominant value $\tilde{D}_{\text{CJ}}/\tilde{M}_{0\text{CJ}}^2 \equiv c_0/\tilde{M}_{0\text{CJ}}$, and it can be used to express one solution with the other,

$$\frac{p_{\text{CJc}} - p_{\text{CJx}}}{p_{\text{CJc}}} = \frac{1 - M_{0\text{CJc}}^{-4}}{1 + M_{0\text{CJc}}^{-2}/\bar{\gamma}} = 1 - (M_{0\text{CJc}}^{-2}/\bar{\gamma}) + \mathcal{O}(M_{0\text{CJc}}^{-2}/\bar{\gamma})^2, \quad (94)$$

$$\frac{v_{\text{CJx}} - v_{\text{CJc}}}{v_{\text{CJx}}} = \frac{1 - M_{0\text{CJc}}^{-4}}{1 + \bar{\gamma}M_{0\text{CJc}}^{-2}} = 1 - (\bar{\gamma}M_{0\text{CJc}}^{-2}) + \mathcal{O}(\bar{\gamma}M_{0\text{CJc}}^{-2})^2. \quad (95)$$

A.3. There are two overdriven detonation solutions ($Q_0 > 0$, $D \geq D_{\text{CJc}}$, figure 2-left); only the upper (U) is a physical intersect of a Rayleigh-Michelson line (8-a) and the equilibrium Hugoniot (90), that is, subsonic ($M < 1$, Subsects.2.3 and 2.4), and it writes

$$\frac{v}{v_0}(D, v_0, p_0) = \frac{\bar{\gamma} - \sqrt{\Delta_D} + M_0^{-2}}{\bar{\gamma} + 1}, \quad \frac{v_0 p}{D^2} = \frac{1 + \sqrt{\Delta_D} + M_0^{-2}/\bar{\gamma}}{\bar{\gamma} + 1}, \quad (96)$$

$$\Delta_D = \left(1 - \left(\frac{D_{\text{CJc}}}{D} \right)^2 \right) \left(1 - \left(\frac{D_{\text{CJx}}}{D} \right)^2 \right) = (1 - M_0^{-2})^2 - \left(\frac{\tilde{D}_{\text{CJ}}}{D} \right)^4. \quad (97)$$

The lower (L), obtained by changing the sign before $\sqrt{\Delta_D}$ above, is non-physical because it is supersonic ($M > 1$). Both reduce to the shock solution (N) by setting $Q_0 = 0$ in (96), that is, $\sqrt{\Delta_D} = 1 - M_0^{-2}$.

From (93), $(D_{\text{CJx}}/D)^2 = (c_0^2/DD_{\text{CJc}})^2 \leq M_{0\text{CJc}}^{-4} \ll 1$ that negligibly contributes to Δ_D compared with $(D_{\text{CJc}}/D)^2$. The typical values $c_0 = 300$ m/s and $D_{\text{CJc}} = 2000$ m/s give the unrealistically small value $D_{\text{CJx}} = 45$ m/s. More generally, this theoretical CJ deflagration viewed as an adiabatic discontinuity with same initial state as the CJ detonation is not admissible because it is subsonic: $M_{0\text{CJx}} < 1$, (9) is not satisfied (Subsect.2.2, App.B). Its usefulness here is only completeness and a simpler writing of relations (96-97), which thus reduce more obviously to the CJ relations (17) if $\Delta_D = 0$, that is, to v_{CJc} and p_{CJc} if $D = D_{\text{CJc}}$, or to v_{CJx} and p_{CJx} if $D = D_{\text{CJx}}$.

Appendix B. Chapman-Jouguet admissibility

B.1. The expanding equilibrium flow behind a self-sustained CJ front is homentropic and self-similar (Subsect.3.1). The backward-facing Riemann invariant is thus uniform, that is, $du - (v/c) dp = 0$, and, since $u_p < u_{\text{CJ}}$, the material speed u (as well as p and v^{-1}) and the frontward-facing perturbation velocity $u + c = x/t$ must decrease from the CJ front so that expansion can spread out. Thus, differentiating $u + c$ and expressing p and c as functions of s and v give $d(u + c) = \Gamma du = -\Gamma v dp/c = cdv/v$ [29], hence the constraint $\Gamma > 0$. Similarly, T decreases from the CJ front if $G > 0$ (3).

B.2. Using (13-b), the second-order differentials of $h(s, p)$, $p(s, v)$ and the Hugoniot relation give

$$\left. \frac{F_{\text{CJ}}}{2} \frac{\partial^2 p_{\text{H}}}{\partial v^2} \right)_{\text{CJ}} = \left. \frac{\partial^2 p_{\text{S}}}{\partial v^2} \right)_{\text{CJ}} = 2 \left(\frac{D_{\text{CJ}}}{v_0} \right)^3 \frac{\Gamma_{\text{CJ}}}{D_{\text{CJ}}}, \quad (98)$$

$$\left. \frac{v_0^2 T_{\text{CJ}}}{D_{\text{CJ}}^2} \frac{\partial^2 s_{\text{R}}}{\partial v^2} \right)_{\text{CJ}} = -2 \frac{\Gamma_{\text{CJ}}}{G_{\text{CJ}}}, \quad \left. \frac{v_0^2 T_{\text{CJ}}}{D_{\text{CJ}}^2} \frac{\partial^2 s_{\text{H}}}{\partial v^2} \right)_{\text{CJ}} = 2 \left(\frac{v_0}{v_{\text{CJ}}} - 1 \right) \frac{\Gamma_{\text{CJ}}}{F_{\text{CJ}}}, \quad (99)$$

which show that $F_{\text{CJ}} \neq 0$ (Subsect.3.2) is also the condition for the Hugoniot curvature and the entropy variations to be finite at a CJ point for physical isentropes ($\Gamma \neq 0$, Subsect.3.4): 2 isentropes cannot have a same CJ contact point. The curvatures of a Hugoniot and an isentrope have the same sign if $F_{\text{CJ}} > 0$, that is, if $G_{\text{CJ}} < 2/(v_0/v_{\text{CJ}} - 1)$, that of the Hugoniot being the larger if $0 < G_{\text{CJ}} < F_{\text{CJ}} < 2/(v_0/v_{\text{CJ}} - 1) < 2$, which is the case for most fluids.

B.3. Using (14-b) and (59), the derivative of M with respect to v along a Hugoniot at a CJ point is

$$\left. \frac{\partial M_{\text{H}}}{\partial v} \right)_{\text{CJ}} = \frac{\Gamma_{\text{CJ}}}{v_{\text{CJ}}}, \quad (100)$$

which shows, since $\Gamma_{\text{CJ}} > 0$, that $M < 1$ above, and $M > 1$ below, a CJ point, hence $F_{\text{CJ}} > 0$, $\partial^2 p_{\text{H}}/\partial v^2)_{\text{CJ}} > 0$ and $\partial^2 s_{\text{H}}/\partial v^2)_{\text{CJ}} > 0$ from (98) and (99). Also, comparing the slopes of a Rayleigh-Michelson line, a Hugoniot and an isentrope (10)-(11) about a CJ point with $\Gamma > 0$ indicates that $0 < F < 2$ if $G > 0$, and $F > 2$ if $G < 0$. Therefore, a CJ point is physically admissible only on a convex Hugoniot arc, excluding its meeting point with a concave arc where Γ_{CJ} should then be zero; and s increases and M decreases with decreasing v , so the physical branch of this arc is above the CJ point. Other derivations involve concavity of entropy $s(e, v)$ or equivalently convexity of energy $e(s, v)$.

Appendix C. A model problem

C.1. Let the differentials of the functions $\beta(w, x)$ and $\sigma(w, x)$ of the two variables w and x satisfy

$$\varepsilon d\beta = adw + bdx, \quad (101)$$

$$d\sigma = qdw + rdx, \quad (102)$$

where ε, a, b, q, r are finite functions of β, w and x . These relations define the constraints

$$\varepsilon \left(\frac{\partial \beta}{\partial x} \right)_w = b, \quad \varepsilon \left(\frac{\partial \beta}{\partial x} \right)_\sigma = a \left(\frac{\partial w}{\partial x} \right)_\sigma + b, \quad 0 = q \left(\frac{\partial w}{\partial x} \right)_\sigma + r. \quad (103)$$

The last, (103-c), is the triple product rule, which follows from (102) being a total differential,

$$d\sigma = \left(\frac{\partial \sigma}{\partial w} \right)_x dw + \left(\frac{\partial \sigma}{\partial x} \right)_w dx \Rightarrow \left(\frac{\partial \sigma}{\partial x} \right)_w = - \left(\frac{\partial \sigma}{\partial w} \right)_x \left(\frac{\partial w}{\partial x} \right)_\sigma \Leftrightarrow r = -q \left(\frac{\partial w}{\partial x} \right)_\sigma. \quad (104)$$

Therefore, if either $\partial w / \partial x)_\sigma$ or $\partial \sigma / \partial x)_w \equiv r$ is zero, so is the other if $\partial \sigma / \partial w)_x \equiv q$ is finite and non-zero.

C.2. In the limit $\varepsilon = 0$, denoted by the superscript (ε) ,

$$(103\text{-a}) \text{ shows that } b^{(\varepsilon)} = 0 \text{ if } \left(\frac{\partial \beta}{\partial x} \right)_w^{(\varepsilon)} \text{ is finite,} \quad (105)$$

$$\text{then (103-b) shows that } \left(\frac{\partial w}{\partial x} \right)_\sigma^{(\varepsilon)} = 0 \text{ if } \left(\frac{\partial \beta}{\partial x} \right)_\sigma^{(\varepsilon)} \text{ is finite and } a^{(\varepsilon)} \text{ is finite and } \neq 0, \quad (106)$$

$$\text{then (103-c) shows that } \left(\frac{\partial \sigma}{\partial x} \right)_w^{(\varepsilon)} \equiv r^{(\varepsilon)} = 0 \Leftrightarrow \left(\frac{\partial w}{\partial x} \right)_\sigma^{(\varepsilon)} = 0 \text{ if } q^{(\varepsilon)} \equiv \left(\frac{\partial \sigma}{\partial w} \right)_x^{(\varepsilon)} \text{ is finite and } \neq 0. \quad (107)$$

The constraints above and (104) thus imply the equivalence $(d\sigma)^{(\varepsilon)} = 0 \Leftrightarrow (dw)^{(\varepsilon)} = 0$, but not that $(d\sigma)^{(\varepsilon)}$ or $(dw)^{(\varepsilon)}$ is zero. The DSI theorem (Subsect.3.3) is the application for which $\varepsilon = 1 - M$, $\sigma = s$, $\beta = v, p$ or h , $w = D$, $x = v_0$, $a \propto K_z \neq 0$, $q \propto K_s \neq 0$, $b \propto \Phi_z^*$ and $r \propto \Phi_s^*$.

C.3. If the arguments of $b(\beta, w, x)$ and $r(\beta, w, x)$ include the same grouping $\mu_0(\beta, w, x)$, and if conditions exist for which $(d\sigma)^{(\varepsilon)} = 0$ or $(dw)^{(\varepsilon)} = 0$, eliminating μ_0 between the constraints $b^{(m)} = 0$ and $r^{(\varepsilon)} = 0$ defines a compatibility relation between β, w and x , that is,

$$b^{(\varepsilon)}(\beta, w, x, \mu_0) = 0 \quad \text{and} \quad r^{(\varepsilon)}(\beta, w, x, \mu_0) = 0 \quad \Rightarrow \quad \beta = \beta^{(\varepsilon)}(w, x), \quad (108)$$

which then returns $\mu_0^{(\varepsilon)}$ by substituting $\beta^{(\varepsilon)}$ for β in either of these constraints. These are the operations in Subsection 3.4 that give v_{CJ}/v_0 and dp_0^*/dv_0 , here represented by μ_0 .

References

- [1] Jouguet, E. 1901 Sur la propagation des discontinuités dans les fluides, *C. R. Acad. Sci. Paris*, 132, 673-676.
- [2] Jones, H. 1949 The properties of gases at high pressures that can be deduced from explosion experiments, *3rd Symp. on Combustion, Flame and Explosion Phenomena*, Williams and Wilkins, Baltimore, 590-594.
- [3] Stanyukovich, K. P. 1960, *Non-stationary flows in continuous media*, Pergamon Press, London (transl. State Publishers of Technical and Theoretical Literature, Moscow, 1955).
- [4] Manson, N. 1958 Une nouvelle relation de la théorie hydrodynamique des ondes de détonation, *C. R. Acad. Sci. Paris*, 246, 2860-2864.
- [5] Vieille, P. 1900 Rôle des discontinuités dans la propagation des phénomènes explosifs, *C. R. Acad. Sci. Paris*, 130, 413-416.
- [6] Sharpe, G. J. 2000 The structure of planar and curved detonation waves with reversible reactions, *Phys. Fluids*, 12(11), 3007-3020.
- [7] Higgins, A. 2012 Steady one-dimensional detonation, in *Shock Waves Sciences and Technology Reference Library, Vol.6: Detonation dynamics*, Springer-Verlag Berlin Heidelberg, 33-105.
- [8] Tarver, C. M. 2003 On the existence of pathological detonation waves, *13th APS Topical Conf. on Shock Compression of Condensed Matter*.
- [9] Tarver, C.M. 2010 Chemical energy release in several recently discovered detonation and deflagration flows, *Journal of Energetic Materials*, 28:sup1, 1-15.
- [10] Wood, W. W., Kirkwood, J. G. 1954 Diameter effect in condensed explosives. The relation between velocity and radius of curvature of the detonation wave, *J. Chem. Phys.*, 22(11), 1920-1924.
- [11] He, L., Clavin, P. 1994 On the direct initiation of gaseous detonations by an energy source, *J. Fluid Mech.*, 277, 227-248.
- [12] Kasimov, A. R., Stewart, D. S. 2004 On the dynamics of self-sustained one-dimensional detonations: a numerical study in the shock-attached frame, *Phys. Fluids*, 16(10), 3566-3578.
- [13] Short, M., Voelkel, S. J., Chiquete, C. 2020 Steady detonation propagation in thin channels with strong confinement, *J. Fluid Mech.* 889, A3.
- [14] Zel'dovich, Ya. B., Kompaneets, A. S. 1960 *Theory of detonation*, Academic Press, New York (transl. Gostekhizdat, Moscow, 1955).
- [15] Dremin, A. N. 1999 *Towards detonation theory*, Springer, New York.
- [16] Tarver, C. M. 2012 Condensed matter detonation: theory and practice, in *Shock Waves Sciences and Technology Reference Library, Vol.6: Detonation dynamics*, Springer-Verlag Berlin Heidelberg, 339-372.
- [17] Berger, J., Viard, J. 1962 *Physique des explosifs solides*, Dunod, Paris.
- [18] Bastea, S. 2017 Nanocarbon condensation in detonation, *Nature, Scientific Reports*, 7, 42151.
- [19] Edwards, L., Short, M. 2019 Modeling of the cellular structure of detonation in liquid explosives, *APS Division of Fluid Dynamics*, abstract H05.008.
- [20] Denisov, Yu. N., Troshin, Ya. K. 1959 Pulsating and spinning detonation of gaseous detonation in tubes, *Dokl. Akad. Nauk. SSSR*, 125, 110-113.
- [21] Desbordes, D., Presles, H.-N. 2012 Multi-scaled cellular detonation, in *Shock Waves Sciences and Technology Reference Library, Vol.6: Detonation dynamics*, Springer-Verlag Berlin Heidelberg, 281-338.
- [22] Urtiew, P. A., Kusubov, A. S. 1970 Wall traces of detonation in nitromethane-acetone mixtures, *5th Symp. (Int.) Detonation*, ONR, 105-114.
- [23] Persson, P. A., Bjarnholt, G. 1970 A photographic technique for mapping failure waves and other instability phenomena in liquid explosives detonation, *5th Symp. (Int.) Detonation*, ONR, 115-118.
- [24] Tarver, C. M., Urtiew, P. A. 2010 Theory and modeling of liquid explosive detonation, *Journal of Energetic Materials*, 28(4), 299-317.
- [25] Fickett, W., Davis, W. C. 2000 *Detonation: theory and experiment*, Dover Publications, Inc.
- [26] Duhem, P. 1909 Sur la propagation des ondes de choc au sein des fluides, *Z. Phys. Chem.*, 69, 160-186.
- [27] Bethe, H. A. 1942 The theory of shock waves for an arbitrary equation of state, *OSRD Report 545*.

- [28] Weyl, H. 1949 Shock waves in arbitrary fluids, *Comm. Pure Appl. Math.*, 2, 103-122.
- [29] Thomson, P. A. 1971 A fundamental derivative in gasdynamics, *Phys. Fluids*, 14(9), 1843-1849.
- [30] D'yakov, S. P. 1954 On the stability of shock waves, *Zh. Eksp. Teor. Fiz.*, 27, 288-295.
- [31] Kontorovich, V. M. 1957 *JETP*, 6(6): Concerning the stability of shock waves, 1179-1180, and Reflection and refraction of sound by a shock wave, 1180-1181.
- [32] Bates, J. W., Montgomery, D. C. 2000 The D'yakov-Kontorovich instability of shock waves in real gases, *Phys. Rev. Letters*, 84(6), 1180-1183.
- [33] Brun, L. 2013 The spontaneous acoustic emission of the shock front in a perfect fluid: solving a riddle, CEA report CEA-R-6337.
- [34] Clavin, P., Searby, G. 2016 *Combustion waves and fronts in flows: flames, shocks, detonations, ablation fronts and explosion of stars*, Ed. Cambridge University Press, ISBN 10: 1107098688.
- [35] Landau, L. 1944, cit. in Landau L. & Lifchitz E., *Fluid mechanics*, Chapt.IX, §88, Pergamon, Oxford,1958.
- [36] Lax, P. D. 1957 Hyperbolic systems of conservation laws, II, *Comm. Pure and Appl. Math.*, 10, 537-566.
- [37] Fowles, G. R. 1975 Subsonic-supersonic condition for shocks, *Phys. Fluids*, 18(7), 776-780.
- [38] Gordon, S., McBride, B. J. 1994 Computer program for calculation of complex chemical equilibrium compositions and applications, I. Analysis. NASA Reference Publication 1311.
- [39] Taylor, G. I. 1950 (1941) The dynamics of the combustion products behind plane and spherical detonation fronts in explosives, *Proc. Roy. Soc.*, A 200, 235-247.
- [40] Döring, W., Burkhardt, G. 1944 Beiträge zur Theorie der Detonation, *Deutsche Luftfahrtforschung*, Bericht n°1939.
- [41] Davis, W. C. 1981 Equation of state from detonation velocity measurements, *Comb. and Flame*, 41, 171-178.
- [42] Wood, W. W., Fickett, W. 1963 Investigation of the CJ hypothesis by the "Inverse Method", *Phys. Fluids*, 6 (5), 648-652.
- [43] Wecken, F. 1959 Note Technique n°459 (avril), Institut Franco-Allemand de Saint-Louis.
- [44] Sheffield, S. A., Davis, L. L., Engelke, R., Alcon, R. R., Baer, M. R., Renlund, A. M. 2001 Hugoniot and shock initiation studies of isopropyl nitrate, 12th APS Topical Conf. on Shock Compression of Condensed Matter.
- [45] Zhang, F., Murray, S. B., Yoshinaka, A., Higgins, A. 2002 Shock initiation and detonability of isopropyl nitrate, 12th Symp. (Int.) Detonation, San Diego, CA, ONR, 781-790.
- [46] Brochet, C., Fisson, F. 1970 Determination de la pression de détonation dans un explosif condensé homogène, *Explosifs*, n°4, 113-120 (1969), and Monopropellant detonation: isopropyl nitrate, *Astronaut. Acta*, 15, 419-425.
- [47] Davis, W. C., Craig, B. G., Ramsay, J. B. 1965 Failure of the Chapman-Jouguet theory for liquid and solid explosives, *Phys. Fluids*, 8(12), 2169-2182.
- [48] Lysne, P. C., Hardesty, D. R. 1973 Fundamental equation of state of liquid nitromethane to 100 kbar, *J. Chem. Phys.*, 59(12), 6512-6523.
- [49] Jones, W. M., Giauque, W. F. 1947 The entropy of nitromethane. Heat capacity of solid and liquid. Vapor pressure, heats of fusion and vaporization, *J. Am. Chem. Soc.*, 69(5), 983-987.
- [50] Berman, H. A., West, E. D. 1967 Density and vapor pressure of nitromethane 26° to 200° C, *J. Chem. and Eng. Data*, 12(2), 197-199.
- [51] Bernard, Y., Brossard, J., Claude, P., Manson, N. 1966 Caractéristiques des détonations dans les mélanges liquides de nitropropane II avec l'acide nitrique, *C. R. Acad. Sci. Paris*, 263, 1097-1098.
- [52] Garn, W. B. 1960 Detonation pressure of liquid TNT *J. Chem. Phys.*, 32(3), 653-655.
- [53] Garn, W. B. 1959 Determination of the unreacted Hugoniot for liquid TNT, *J. Chem. Phys.*, 30(3), 819-822.
- [54] Chiquete, M., Short, M. 2019 Characteristic path analysis of confinement influence on steady two-dimensional detonation propagation, *J. Fluid Mech.*, 863, 789-816.
- [55] Petrone, F. J. 1968 Validity of the classical detonation wave structure for condensed explosives, *Phys. Fluids*, (11)7, 1473-1477.